Moulded Electrical Machines and Laminated Windings

Development, Experiment, Realization, and Evaluation

Conny Högmark

Licentiate Thesis
Department of Measurement Technology and Industrial Electrical Engineering

2013

Department of Measurement Technology and Industrial Electrical Engineering
Faculty of Engineering
Lund University
Box 118
221 00 LUND
SWEDEN

http://www.iea.lth.se

ISBN:978-91-88934-58-1
CODEN: LUTEDX/(TEIE-1066)/1-132/(2013)

Printed in Sweden by Media-Tryck, Lund University
Lund 2014

Even a brilliant idea can be wrong

C. Högmark

Abstract

The goal of this thesis is to investigate the possibility of making an electrical machine part in one production step, by moulding a finished stator core together with a winding. As new mouldable core materials are developed, with very low core losses, the opportunity arises for a different approach to the manufacturing of electrical machines. Moulding the stator core potentially allows for decreasing the production cost during the manufacturing process, by minimizing the manual work in the production of the machine. This thesis therefore focuses on simplifying the production of electrical machines, and covers aspects including the different kinds of moulding techniques and winding designs suitable for moulding.

When moulding an electrical machine, it is possible to create a complex 3D core in the stator, during moulding the core forms in the available space the winding in the mould don’t occupy. This creates challenges in the winding design and means that it is essential to control the geometrical form of the winding in order to achieve the intended result of the moulding. The closeness of the core to the winding also benefits the thermal dispersion in the machine, but can affect the dielectrical strength in the machine.

This thesis describes a number of practical winding experiments performed in pursuit of a deeper understanding of winding design for moulded machines. The experiments build an understanding of winding configuration and its impact on the performance of the moulded machine.

In addition to these experiments, a generator intended for automotive applications was designed and prototyped. This generator is a three-phase axially stacked machine with an electrically magnetized rotor. A few different stator segments were prototyped and evaluated. In addition, different multi-turn windings were used: two hand-made windings and a pressed winding made in a fixture. The results of the evaluation are presented, and an additional investigation and discussion of the design is made based on the evaluation results.

During the intensive winding investigation, a laminated winding was invented. This type of winding gives good geometrical tolerances, and has a high conductor fill factor as a result of an easy manufacturing process, making it a perfect winding for moulding. Furthermore, the winding production process allows selection of the conductor fill factor in the winding, which in turn makes direct cooling possible. The possibility for an enhanced cooling directly in the winding slot is a very interesting aspect of this winding. Several prototypes of the winding were made, and the possibilities for enhanced cooling were tested.

Acknowledgements

Finishing this thesis has been a struggle but with support and a lot of idea bouncing with Avo Reinap together with the determination of my supervisor Mats Alaküla that I finish this licentiate thesis, the thesis is now at its end. As I write these last words there are a number of people and organisations that have contributed in some way to my work and I want to thank them, they are Vinova, Magcomp AB, ABVolvo, Proviking research school, department of Industrial production in Lund university and last but not the least my co-workers at the division IEA in Lund university where Getachew Darge should be especially recognised. Kenneth Frogner is another I want to mention as he introduced me in to flying with a paraglider and this has enriched my life and he also have been a good listener to some of my craziest ideas.

Lund, 21 August 2013
Conny Högmark

Contents

Chapter 1

Introduction

1.1 Background

When work began on this licentiate thesis, there was a great deal of interest in moulding electromagnetic energy converters, and these are still of interest in several applications. The moulding technique has the potential to make energy-efficient and production-friendly electrical machines, and the goal of the present thesis is to advance this technique in order that electrical machine production can take a step forward in evolution. During the thesis work, the focus moved from the moulding techniques and their practical realization in electrical machine production towards production-friendly winding designs for moulded electrical machines as well as unconventional winding designs and applications. This change of research focus was actually due to the early discovery of winding utilization problems in geometric accuracy, production-friendliness, and copper fill factor, and was necessary if the intended research goal was to be achieved.

After extensive hours of experimental work, design, and analysis of the results, the idea of laminated winding was developed. The idea came to me in a car on a snowy dark road with my two friends and colleagues Avo Reinap and Kenneth Frogner. Since then, my research has focused on the potential of laminated winding, and so this thesis covers my results from the development of winding and moulding production methods, through the design of electrical machines, to the production of electrical machines.

1.2 Objectives

The objective of this thesis is to describe production methods that contribute to a production-friendly environment and solutions for using soft magnetic mouldable composite (SM^2C) core materials in electrical machines. The aspects discussed include winding arrangements, design, and practical constructions for moulds and electrical machines. The thesis also includes the production and validation of a variety of moulded powder core electrical machines with a focus on manufacturability and performance.

This thesis also discusses the usability of SM^2C materials in the design of electrical machines, and considers in which applications the material will utilize its potential. The potential and utilization of the laminated winding technique are described, and several prototypes and measurement results of the laminated winding are shown.

1.3 Outline of the Thesis

Chapter 2 gives an overview of the moulding technique, and explains why moulding could be beneficial in building electrical machines. SM^2C materials are described, and the different kinds of iron compression moulding techniques are discussed. One of the most important aspects of moulding (and one that is very easy to forget) is the design of the mould, which is also described here.

Chapter 3 describes winding design goals and a number of winding geometric layouts along with their suitability (or lack thereof) for moulding. It also presents winding configurations for moulding, such as circumferentially distributed windings and axially distributed windings.

Chapter 4 describes a number of winding experiments and the experimental platform that was used. These experiments were performed to get a deeper understanding of the winding design for machines moulded with SM^2C, and to understand the impact of winding configuration on the performance of the moulded machine. This chapter summarizes the knowledge and understanding gained during these experiments and knowledge from prior machine prototypes with SM^2C.

Chapter 5 is divided into three parts:

1) The electromagnetic design, including stator segment design and rotor design.

2) A thermal investigation comparing the existing generator design with the three electromagnetic designs that fulfil the requirements.

3) Prototyping the generator with three different stator windings and an electromagnetic rotor.

Chapter 6 is divided into two parts, the first of which gives the results of tests on moulded dummy windings and the two moulded segments. Some unanswered questions came up during these tests, and so the second part of the chapter consists of further analysis and discussion of the design of the generator.

Chapter 7 gives a full view of laminated winding: background, production, thermal advantages, and material selection for the laminated winding. The possibility of a rapid cooling is also presented.

Chapter 8 comprises conclusions and suggestions for future work.

1.4 Contributions

The main contribution of this thesis is the investigation of the possibility to incorporate windings in the making of the stator by moulding the stator iron core in electrical machines.

This thesis explains the winding configurations suitable for moulding the stator in electrical machines and explains a number of guidelines for the design of the mould.

This thesis investigates the possibility of a moulded stator for generators in heavy vehicles both in design and in experimental work.

This thesis also investigates the new laminated winding and its promising feature in rapid cooling by forcing air thru the lamination of the winding.

1.5 Publications

Reinap, A., Hagstedt, D., Högmark, C., Alaküla, M. (2012). Sub-optimization of a claw-pole structure according to material properties of soft magnetic materials. *IEEE Transactions on Magnetics*, vol. 48, no. 4, pp. 1681-1684.

Andersson, R., Högmark, C., Reinap, A., Alaküla, M. (2012). Modular three-phase machines with laminated winding for hybrid vehicle applications. *International Electric Drives Production Conference and*

Exhibition (EDPC 2012), Nuremberg, Germany, 16–17 October 2012.

Högmark, C., Reinap, A., Frogner, K., Alaküla, M. (2012). Laminated winding with rapid cooling capability for electrical machines. *International Conference for Inductive and Electromagnetic Components, Systems and Devices including Manufacturing and Processing (INDUCTICA 2012),* Berlin, Germany, 26–28 June 2012.

Högmark, C., Andersson, R., Reinap, A., Alaküla, M. (2012). Electrical machines with laminated winding for hybrid vehicle applications. *International Electric Drives Production Conference and Exhibition (EDPC 2012),* Nuremberg, Germany, 16–17 October 2012.

Svensson, L., Frogner, K., Reinap, A., Högmark, C., Andersson, M., Alaküla, M. (2012). Alternative production process for electric machine windings. *International Electric Drives Production Conference and Exhibition (EDPC 2012),* Nuremberg, Germany, 16–17 October 2012.

Reinap, A., Hagstedt, D., Högmark, C., Alaküla, M. (2011). Evaluation of a semi claw-pole machine with SM^2C core. *International Electrical Machines and Drives Conference (IEMDC 2011)*, Niagara Falls, Ontario, Canada, 15–18 May 2011.

Reinap, A., Högmark, C., Alaküla, M., Cedell, T., Andersson, M. (2010). An integrated design of SM^2C core motor for vehicular applications. *International Conference on Electrical Machines (ICEM 2010),* Rome, Italy, 6–8 September 2010.

Reinap, A., Högmark, C., Alaküla, M., Cedell, T., Andersson, M. (2010). Prototype based study of different winding configurations with SM^2C core. *International Conference on Electrical Machines (ICEM 2010),* Rome, Italy, 6–8 September 2010.

Reinap, A., Högmark, C., Alaküla, M., Cedell, T., Andersson, M., Jeppsson, P. (2008). Design and prototyping a torus machine with a rotocast core. *International Conference on Electrical Machines (ICEM 2008)*, Vilamoura, Portugal, 6–9 September 2008.

Cedell, T., Jeppsson, P., Andersson, M., Ståhl, J.-E., Högmark, C., Reinap, A., Alaküla, M. (2009). New advances in soft magnetic materials - properties of moulded flux conductors in inductors and electrical motors. *Inductica Technical Conference (CWIEME 2009),* Berlin, Germany, 5–7

May 2009.

Chapter 2

Moulding electrical machines

This chapter covers the challenges related to a production process which uses soft magnetic composite powder to mould the magnetic core of electrical machines. The moulding techniques used to create this magnetic core (i.e. the “conductor” for the magnetic field in electrical machines) are described. The chapter also includes an explanation of why moulding can be beneficial in the manufacturing process of electrical machines.

2.1 Different core materials

Electrical machines are built with a structure of electrical and magnetic conductors. The magnetic conductors, usually called the core of the electrical machine, should have high magnetic permeability; that is, they should be much better magnetic conductors than air, and have low or no losses related to magnetic flux variations.

Core materials based on iron are used due to the high magnetic permeability of iron, which at its best is several thousand times better than air. To limit the losses related to flux variations, the iron is alloyed with other metals and split into sheets isolated from each other in a direction perpendicular to the flux direction, the latter to reduce eddy current induction. There is a limitation on how thin the sheets can be while still being capable of being manufactured at a low cost. When the thickness of the sheets is decreased, the insulation layer becomes a relatively larger part of the sheet’s final thickness, and this leads to a decreased iron fill factor in the core.

To decrease the core losses, it is also possible to use iron powder pressed together with a binder. These composites are generally called soft magnetic composites (SMC). However, the advantage of reduced core losses is accompanied by decreased permeability compared to a laminated core. Since SMC material is pressed, there are also limitations on the possible geometric shapes of the pressed SMC parts.

A special form of SMC is the soft magnetic mouldable composite (SM^2C). In comparison to pressed SMC, SM^2C is characterized by having a large enough binder content that the mixture is able to flow into a mould. As will be shown in this thesis, the resulting iron density in the moulded core can be increased significantly, compared to the iron content in the moulding mix, by an intentional use of gravitation or of extended gravitation via centrifugation.

The use of SM^2C makes it possible to create the intended geometric shape of the core and reduce the core losses further, but again at the cost of permeability. Figure 2.1 gives a comparison of the relative permeability of different core materials.

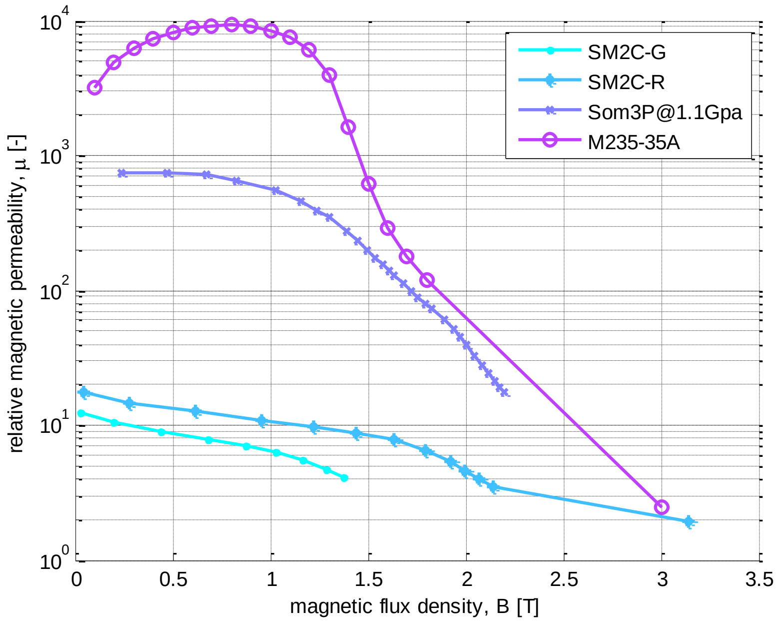

Figure 2.1 Differences in permeability of four different core materials. M235-35A is laminated sheets, Som 3P @ 1.1GPa is an SMC material, and SM^2C-R and SM^2C-G are two SM^2C materials.

2.2 Why moulding?

There are already several high-performing materials for conducting magnetic flux, and so it could be asked why there is a need to introduce yet another; can SM^2C bring new and useful material parameters for machine construction? The material has a low capability to conduct magnetic flux, with a relative permeability μ_r around 15 times larger than the permeability of air. This number can be compared to laminated steel, which has a μ_r equal to 8000, and SMC materials, which have a μ_r that peaks at 800 [2].

The explicit answers to the question of “why moulded cores?” are divided between two major discussion points: I) the production of the electrical machine, and II) the electromagnetic design and function of the flux conductor.

From a manufacturing point of view, the moulding process introduces the possibility for an automated process to produce a large number of items per unit of time. From an electromagnetic point of view, moulded cores have a considerably higher permeability then air and considerably lower core losses than other core materials commonly used today. These aspects mean that SM^2C materials are highly appealing for electromagnetic component production. They are further discussed in the next sections.

Why moulding?

Production	**Electromagnetic**
• Automation-friendly	• Low permeability
• Integration of sensors, driver applications, cooling, and so on	• High power density
• Decreased production costs	• Low AC losses
• Simplified winding	• Substantially increased

production	electrical frequency
• Fewer processing steps	• Decreased impact of magnetic saturation
	• Complex 3D flux conductors

Electromagnetic design

Low permeability. The bulk permeability of SM^2C is significantly lower than that of most other core materials, typically with a relative permeability $\mu_r < 20$. This leads to a preference for short magnetic flux paths in circuits with large air gaps, to limit the impact of this low permeability.

Complex 3D core shapes. The ability to mould the core makes it easy to create complex core shapes. This can be used to simplify the winding design, as long as the permeability limitations are taken into account.

Low magnetization losses/high excitation frequency. The core losses of SM^2C are very low – from the point of view of traditional electrical machine design, they are almost non-existent up to fundamental frequencies of tens of kilohertz. This opens up the possibility to run machines at high fundamental frequencies and thus obtain high power densities. Since low permeability may cause high leakage inductances, high reactive voltage drops at high frequencies must be considered.

Production

Automation friendly. The SM^2C moulding process is ideal for automated production. The production steps consist of I) filling the mould, II) centrifugation to increase the density, III) thermal acceleration of the hardening process, and IV) cooling.

Integration. Other elements can be introduced in the moulding process, such as the stator winding, primitive pieces of other core materials, sensors, thermal conductors, fastening elements, and so on. This further contributes to efficient production, since many aspects of a machine design can be finished in the same moulding step.

Simplified winding production. In laminated machines, the assembled core acts like a “bobbin” for the windings, and thus the windings are not required to have a certain consistency in shape prior to insertion in the core. With SM^2C cores, the winding shape must be consistent before the moulding, otherwise the moulding process is likely to distort the winding shape. This requires special attention to the winding design and production in relation to moulding with SM^2C.

Insulation. Since the winding comes in very close contact with the core material, if moulded together with the core, special attention needs to be applied to guarantee the electric isolation capabilities of the moulded machine.

There are some drawbacks in using SM^2C material in electrical machines, both from a production and an electromagnetic point of view, but there are possible solutions or guidelines to minimize their impact.

2.3 Moulding theory

This section describes the manufacturing methods called moulding in this thesis, where the floating substance is filled or forced into the cavities of the mould. The production of SM^2C is described, and four different moulding methods are discussed.

SM^2C

SM^2C is produced by mixing SMC powder with a binder to create a mouldable mixture (see Figure 2.2). The SMC is there to conduct the magnetic flux, and the binder is there to hold the magnetic conductor together and provide lubrication during moulding. Several different kinds of SMC materials are available today, not least those produced by Höganäs. SM^2C should not be confused with the SMC materials produced by Höganäs; the latter are created by high pressure compaction leading to higher iron density, higher permeability, higher losses, and a lower freedom of geometric shape compared to SM^2C.

Figure 2.2 SMC and binder are mixed together to create SM^2C for moulding.

The work described in this thesis does not include development of the SM^2C material for machine cores; it is based on previous material and production development at the Division of Material Engineering and Production, Faculty of Technology, Lund University. The goal here is to increase the understanding of this material and thereby contribute to further development. However, the outcome of the moulding process may be influenced by the premix of the SM^2C powder, the selection of the binder, the moulding technique, the moulding process parameters, and not least the design of the mould. Future improvements of the material composition may improve results, and change some of the conclusions drawn in this thesis.

There are several parameters to consider in the attempt to optimize the SM^2C material for moulding and thereby increase the fill factor of the magnetic flux path. The inputs to the moulding process, techniques, and parameters are described separately below.

The SMC powder

The SMC powder can be described with the following parameters:

- Material combination in the powder and thermal treatment. The alloy used in the powder particles influences both permeability and losses in the final product. The losses are also influenced by heat treatment of the core material.

- Geometric size and shape of the powder particles. The viscosity and ability to fill a mould is influenced by the shape of the particles. The best particle shape for mould filling is spherical, corresponding to gas-atomized powder. Furthermore, the particle sizes in the powder must be optimized in the mixture for the best iron filling factor in the moulded core.

The binder

When selecting the binder for SM^2C, it is necessary to consider several aspects:

- Heat endurance of the binder. This is vital for the mechanical endurance of the machine over time.

- During moulding, the viscosity of the binder at different temperatures plays a large role in the end result. The binder has two major functions during moulding. First, it decreases the friction between the soft magnetic particles and thus increases the fill factor. Second, it slows down the separation process of the main part of the binder and the soft magnetic powder, thereby helping the soft magnetic powder to reach its destination.

- Lead time for the moulding to reach a solid state plays a vital role in the production time of the machine.

- Environmental impact during the moulding process involves both the highly allergenic nature of several binders, and consideration of future recycling of the machine.

During the work with the SM^2C material described in this thesis, the understanding of the magnetic properties in the material has changed. The permeability of the material was initially overestimated, which affected the results of the simulations versus the results from the prototype measurements. Over time, work with the material has corrected this misunderstanding. The development of the understanding of the material is illustrated in Figure 2.3, which shows the different magnetic properties used in simulation and describes the results of prototype production for different SM^2C mixtures. The numbering of the different materials explains the order of the understanding in the material development evaluation.

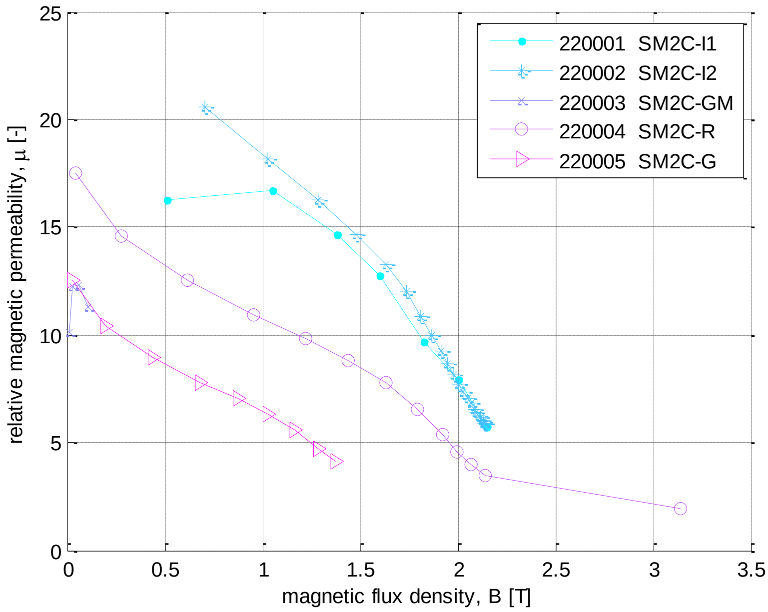

Figure 2.3 SM^{2}C-I1 is the first permeability measurement of the light compressed SM^{2}C material and SM^{2}C-I2 is the second. SM^{2}C-GM is a relative permeability measurement from mixing and moulding with iron powder of size 100µm-200µm, using gravity for compression; this is a mixture for rapid prototyping. At the time of writing, SM2C-R has the "best" material properties achievable. It is produced by the rotocast process with sorted particle sizes and heat-treated powder. SM^{2}C-G is an extrapolation of SM^{2}C-GM based on the shape of the characteristic measurements for SM2C-R.

Moulding techniques

The basic moulding technique is to feed the SM^{2}C material into a mould while in liquid state. The intended components for the finished stator, such as winding, core inserts, and sensors, are placed in the mould prior to moulding. The desired outcome of this procedure is a magnetic core with high density, low mechanical stress, and high electric resistivity in the manufactured part, resulting in a relatively high permeability core with low specific core losses. During the moulding, a local increase of the iron content is accomplished by selection of an optimal premix and local compression of the SMC powder in the SM^2C. Several techniques can be used for moulding and compressing the powder:

- Injection moulding (gives no local increased SMC density)
- Gravity moulding (can increase local SMC density)
- Vibration moulding (boosts previous method)
- Rotational moulding (maximizes local SMC density)

All of these techniques are low-pressure moulding techniques. This means that there will be no deformation of the soft magnetic particles in the compression process [2]. It also means that the size of the iron particles in the SM^2C material will have an increased impact on the end result of the iron content in the magnetic conductor.

The moulding techniques used with SM^2C are different from the high-pressure techniques used to produce SMC materials. In such materials, for example the Somaloy manufactured by Höganäs, the high-pressure compression technique is in one axis, which can give a density of up to 98% of the iron content [2]; this should be compared to the best mouldable techniques which create SM^2C that peaks at a density of 67% [3]. However, SM^2C allows the creation of complex 3D forms for the flux conductor, via the design of the winding and mould. This is less easy when using the high-compression technique in one axis.

Injection moulding

Injection moulding is a production method that uses SMC powder and thermoplastic mixture for the flux conductor. This mixture is injected into a mould under high temperature and pressure, and allows for an iron fill factor of 60% in the flux conductor [2]. The winding can be placed in the mould prior to the injection of the SMC thermoplastic mixture. The foremost advantage of this technique is that it can be realized in a conventional injection moulding machine. The high pressure during the injection makes the iron particles in the mixture act as a grinding material. At the same time, the temperature of the mixture weakens the insulation of the winding. This harsh moulding environment places increased demand on the winding insulation to avoid short-circuits. Although injection moulding is a fast and production-friendly method, its advantages are outweighed by the disadvantages of wear and tear on the winding during the production process and the low relative permeability.

Gravitational force

The gravitational force of the Earth is the simplest and least strenuous way to compress the iron particles. After the winding, sensor, inserts, and other components have been placed in the mould, the SM^2C is fed in to create the magnetic flux pathway. Once the mould is filled, the force of gravity makes the powder particles migrate downwards and thus increase the local iron density in that direction. There are many similarities between the vibration technique and the gravity-moulding technique, and the latter of these is best utilized to achieve a rapid prototype production for testing different electrical machine configurations.

The vibration technique

With the vibration technique, the mould is prepared with the winding and the SM^2C mix is fed inside. When the mixture has settled to a dense iron mass, a vibration force is applied in order to release bound air in the mixture and vibrate the iron particles into an optimum configuration, very much like vibration of concrete in civil engineering. This will increase both the iron density and the relative permeability in the material, and as a result decrease the reluctance in the flux conductor core.

Rotational moulding technique

In the rotational moulding technique (also known as rotocast), a centripetal force is created by rotating the mould at a significant velocity; this accelerates the SM^2C mix toward the inner surfaces of the mould. The iron powder in the mix will then compress at the inside of the mould, and a separation will take place between the iron powder and the redundant part of the binder. Although similar to that seen with gravitational moulding, the separation here is more extended, and thus the core fill factor is higher. There are two major types of rotational moulding techniques:

- Radial compression
- Lateral linear axial compression

With radial compression, the mould rotates around its own central axis. With lateral linear axial compression, the mould rotates around an external axis (Figure 2.4).

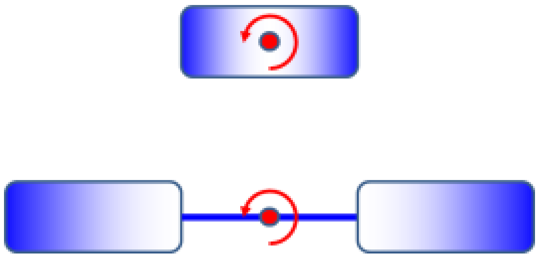

Figure 2.4 Above: radial moulding. Below: lateral linear moulding.

The iron fill factor of the magnetic flux conductor is the most influential property when it comes to achieving the intended torque density in the electrical machine. The maximization of iron fill factor in the moulded component depends on process factors such as centripetal force, compression time, and mould temperature [3], as well as aspects of the mould design. The following aspects are important:

- The centripetal force, which is in the range of 5*g* to 100*g*. Centripetal force is kept low during the filling of the form in radial rotation, and increases in the compacting state.
- The radial difference between the inner and outer parts of the intended SM^2C component. This can affect the iron compaction variations throughout the mould.
- The moulding temperature, which ranges from 20ºC to 80ºC. A higher temperature will accelerate the solidification process, but increasing the temperature will affect the viscosity of the binder, which in turn can affect the ability of the SM^2C to create the intended flux path during moulding.
- The time that the mould spends in rotation; this depends on whether the mould is of an open or closed design. If the mould is of a open design, it can be necessary to continue rotating the mould until the SM^2C mixture reaches a solid state.
- The design of the mould and inserts such as windings. There must be paths for the mixture to flow into and fill the mould; it must not be blocked by these inserts.

The rotocast technique seems to be best utilized in building outer rotor machines, since the SM^2C mix will be geometrically well-defined by the shape of the mould, thus increasing the accuracy of the geometry. If the mould is designed carefully, it is also possible to manufacture inner rotor machines with this technique. An example of a rotocast rig is shown in Figure 2.5.

Figure 2.5 Rotocast rig with a thermal device on top.

2.4 Mould design

Mould designs incorporate several design parameters that will influence the end results of a moulding:

1) The material used in a mould depends on whether the mould will be integrated into the machine, or disassembled, or a combination of both. However, all materials used in the mould must remain stable as the temperature increases. An integrated mould should also use materials that are easy to glue. Conversely, if the mould or part of the mould is designed to be disassembled after moulding, the disassembling parts need to use a material that is difficult to glue.

2) The complexity of assembling and disassembling the mould also has an effect. If the mould is not to be fully integrated in the machine, it needs to have a design that is easy and fast to assemble and disassemble during production. This means that the mould has few parts and the parts have a small release angle in the disassembly direction.

3) Handling of the insert placements is of vital importance in the mould.

4) Handling of the winding connections during moulding is both important and difficult. The difficulty is mostly determined by the winding design.

Materials for moulds

The complexity in mould design can be overwhelming. The level of complexity corresponds to the specific machine design that is intended for moulding. The four points above are examples of considerations in designing moulds.

There are also a number of considerations when it comes to materials for the mould. The major ones are:

1) The size of the mould. The larger the mould is, the more important are the thermal expansion, structural mechanics, and weight of the mould.

2) Possible integration of the mould in the final product. This is one of the more interesting aspects of moulding, and can decrease the number of production steps.

3) How the binder in SM^2C reacts with the mould, and whether the mould needs an added film to stop the SM^2C binding to the mould.

4) The ability of the mould materials to secure repeated geometric accuracy during moulding.

5) Whether the mould will be used once only, or repeatedly.

Several of these considerations can interact; for example, number 1 has a large impact on number 4. Number 4 is the most important consideration when choosing material for the mould. The air gap between the rotor and the stator in the electrical machine is of significant importance, not only in magnetic performance but also in mechanical aspects.

There is a difference between prototype production and an automated production. In prototype production, it is possible to compensate for geometric abnormalities produced during the moulding procedure (e.g. from thermal expansion of the mould's material). This simplifies the selection of material for the mould in prototype and test production. However, the material chosen for test or prototype production may not be appropriate for use in a series production where repetition of geometric tolerances is of highest value.

Mould construction

The physical aspects of mould construction can be divided into three main areas: 1) integration of the mould into the finished product, 2) disassembly of the mould to acquire the finished product, and 3) the choice between one-time or repeated use of the mould.

1) Integration of the mould into the finished product is an interesting aspect of moulding with SM^2C, and worth striving for. This would minimize production costs, as the design of the mould would be identical to the design of the housing of the machine. Some constructions take this to its limit (see Figure 2.6), but most applications require the mould to include a removable part, in order to define the air gap in the finished machine.

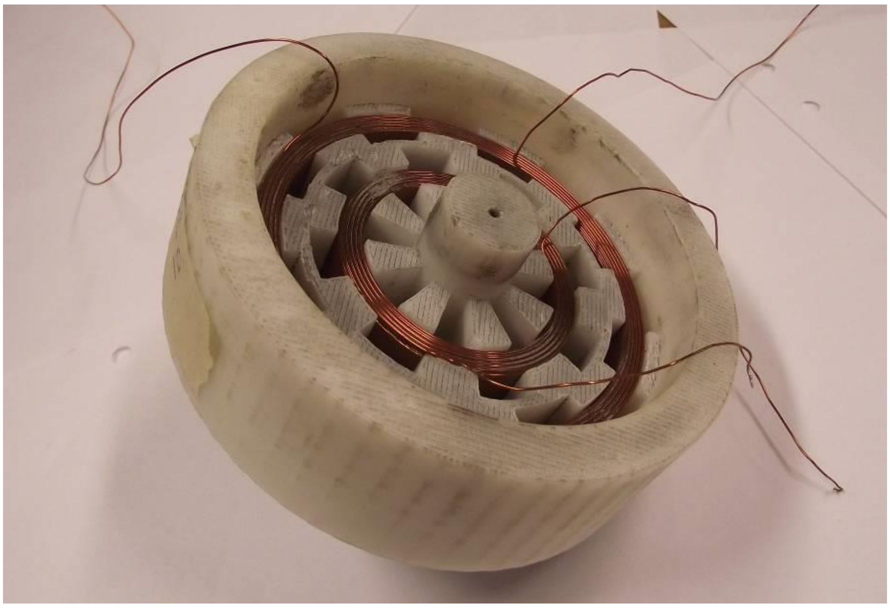

Figure 2.6 An axial flux machine containing no moving parts inside the stator; this means that the stator house is the mould.

2) When the mould needs to be disassembled to some extent in order to collect the moulded product, there are a number of points to consider during the construction:

- The order and direction of the disassembly.
- An angle in the geometry inside of the mould, so it is possible to disassembly the finished product when the moulding have cured.
- Securing the centring of air gap definition in the finished moulded stator, so that the rotor can rotate and have an even air gap between it and the stator.

3) For moulds that will be used only once, there is the option of simplifying the disassembly process by breaking the mould to extract the moulded part. Moulds that will be used repeatedly require more careful handling.

The materials considered for moulds can be divided into two groups, corresponding to moulds that will be disassembled and moulds for one-time use.

Materials for moulds that will be disassembled

As a material for prototypes, the thermoplastic polymer POM-C is excellent. It has several good qualities: for example, it is very hard to glue, it is easy to work with, and it has a low weight. It is stable and stiff, but its high thermal expansion must be taken into consideration before use.

Aluminium can be a good material for moulds, if treated with a coating of Teflon. It is relatively hard to glue, and has a low weight and high strength.

Materials for moulds for one-time use

There are two ways to use the mould as a permanent part of the machine. The first is to use a material that is easy to glue. The second is to manufacture the mould in such a way that the SM^2C will be unable to escape the mould if it is loosened; this can be achieved with a negative angle in the mould/housing. Materials that are easy to glue usually have a low heat conductivity, which can affect the ability to cool the machine. Two materials that can be used in the integration of the mould in the machine are aluminium and glass fibre polyester.

Inserts

One of the more interesting and beneficial aspects of moulding electrical machines is the possibility to place inserts in the mould during moulding, such as windings, parts of other core materials, sensors, cooling circuits, fastening elements, and so on. To handle the inserts during moulding, a number of design configurations need to be considered, depending on which of the four different moulding techniques is to be used. The design configurations to be considered are:

- Control and precision of the winding position during moulding, and handling the winding connections.
- The ability to secure the flow and filling of SM^2C in the mould during moulding.
- Placement control of inserts other than windings, such as sensors, blocks of SMC, and integrated cooling.

2.5 Summary

This chapter describes the basics of moulding principles and different kinds of moulding techniques. There are advantages to all four of the moulding techniques described here, and when it comes to choosing which method is the “best” there must be some consideration of the machine construction and its designed application. For the rotocast technique, outer rotor designs are overrepresented in made prototypes [11] [12]. At the time of writing, only inductors and industry induction heaters use the vibration technique during moulding. The most commonly used compression technique in prototype and winding test production is gravitational compression, due to its simplicity and its capability for a rapid prototype production. This is discussed in more detail in Chapter 4.

Chapter 3

Winding design

When moulding the magnetic core of electrical machines, some properties of the windings that are to be moulded are especially important, such as physical stability and electric isolation. This chapter describes some common winding types for conventional electrical machines, and discusses the arrangement of winding configurations suitable for moulding.

In this context, the term "winding" refers to the electrical stator or rotor circuit in a conventional three-phase electrical machine, such as a radial flux induction machine or a permanently magnetized synchronous machine. It is assumed that the winding arrangement is made in a tooth-slot structure in either the stator or the rotor.

3.1 Winding design goals

When building a machine with the moulding technique, the construction and insulation of the winding has the highest priority. A premade winding gives the possibility to control fill factor, geometry, and insulation of the winding. The main goal is to combine the two major design factors in a premade winding — the physical geometry and the electromagnetic properties of the winding — to achieve a winding with high conductor fill factor and good repeatable geometric shape. Since SM^2C has a low relative permeability, it is necessary to compensate for this with a high fill factor of the winding. This increase in fill factor can be achieved by making the winding design production-friendly by carefully selecting conductor geometry, winding geometry, and production method. When considering production methods, the possibilities to compress a winding to shape in a fixture are very interesting.

3.2 Winding overlapping and coil shapes

The geometric layout of the multiphase winding in a machine can be designed in several different ways; these can be classified in terms of two different groups of coils, overlapping and non-overlapping coils [7]. Overlapping coils are less attractive in moulded machines, as it is difficult to achieve geometric accuracy in the complete winding. Non-overlapping coils are significantly simpler to produce, and offer greater possibilities for achieving the geometric shape necessary for a moulded machine. Figure 3.1 shows several different designs for the winding layout in a machine.

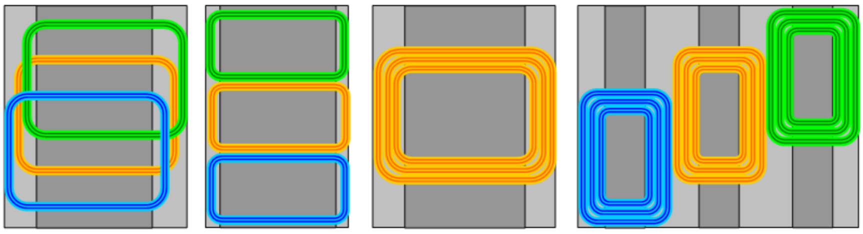

Figure 3.1 From left to right: three-phase overlapping winding, three-phase non-overlapping winding, one-phase winding, and three stacked one-phase windings.

3.3 Windings not suitable for moulding

The stator winding design for traditional three-phase machines is probably the most commonly used winding design in the world (see Figure 3.2).

During moulding of a core, the winding present in the mould is exposed to significant forces when the core material fills the mould and under the compression phase of the core. These forces may wear or damage the winding isolation. For the winding to retain its shape and isolation during the filling of the mould, which may include centrifugation or high pressure injection, it must have a stable shape and be well fixed inside the mould.

This means that traditional winding designs, where the winding is spun “in the air” and then transferred to the tooth-slot structure to be bandaged and impregnated in order to obtain structural integrity, cannot be used in a moulding process.

One example is the distributed winding that can be run in one or more slots, depending on the degree of distribution. Figure 3.2 shows an example of such a distributed three-phase winding. The stator is made of a stack of iron sheets with slots, and acts as a bobbin for the winding. The windings are placed thread by thread in the isolated slots when assembling the stator. The resulting conductor fill factor is around 0.4.

Figure 3.2 Distributed overlapping winding placed in a stator. Here, the stator acts as a bobbin.

3.4 Windings designs suitable for moulding

With traditional windings like the one shown in Figure 3.2, one can say that the core defines the winding via the tooth-slot structure. When moulding a machine, the geometric structure of the winding together with the mould will define the space for the core of the machine. The space in the mould not occupied by the winding will be filled with a material such as SM^2C, thus creating the core of the machine. This places a number of important requirements on the winding:

- The winding must have structural integrity in order to retain its shape and its position in the mould throughout the moulding process.
- The winding must have an insulation layer strong enough to withstand the moulding process and to provide the required isolation in the final product.
- The winding must follow geometric tolerances in order to prevent the core material filling unintended spaces and must retain the specified external dimensions in all cases, even at elevated

temperatures or speeds.

- The winding production method should be simple, low cost, and suitable for automation.

For a SM^{2}C moulded electrical machine, the winding specifications imply that the winding must be carefully designed. There are two aspects of this related to production. The *first* is the quality of the moulded core. During the moulding, the SM^{2}C material will create the core of the machine, and the core geometry will adapt to the cavities of the winding. This behaviour means that the winding design is important for the intended outcome in terms of machine performance (e.g. power conversion). The *second* aspect is that the predetermined coil specifications and constraints must be fulfilled.

It is therefore reasonable to start by looking at a single coil when designing a winding suitable for a moulded machine. The single coil can be simplified to a solenoid as in a claw-pole machine. From a production point of view, as the solenoid has a simple geometry, it enables the highest possible conductor fill factor with the least production effort. However, the low relative permeability of SM^{2}C materials is a hindrance to this kind of machine topology, as the flux leakage will dominate.

This does not hinder the use of solenoid coils in other machine topologies, such as concentrated-winding machines or torus machines. Using a non-overlapping coil structure in the winding makes it possible to increase the control of both the winding geometry and the conductor fill factor. This leads to the goal of the winding design – the least complex production and the highest fill factor achievable. A good example of a machine fulfilling this is the torus machine; see Figure 3.3 [12].

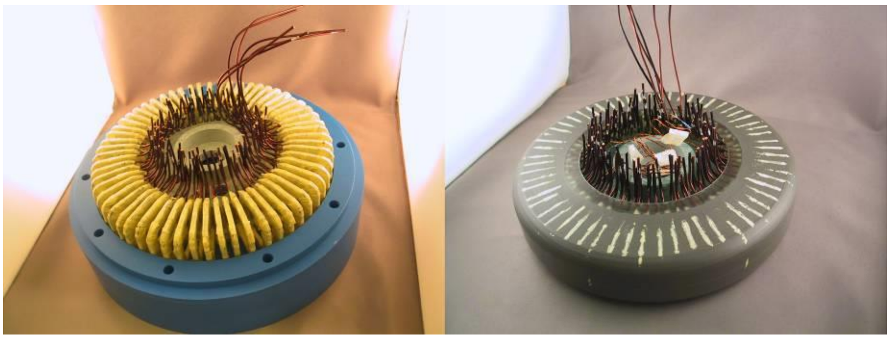

Figure 3.3 Left: A three-phase stator winding made of 60 single solenoid coils. Each coil is simple to make, but a complex geometry can be created by using many coils together. Right: The stator after radial rotocast moulding.

Different winding coil shapes can also be derived from a machine topology where the simple solenoid in a transversal flux machine is formed towards a wave-winding (see Figure 3.4). This not only creates a higher material utilization but also decreases the flux leakage, leading to a higher electromagnetic performance especially in the case of a low-permeability SM^2C core [8][9].

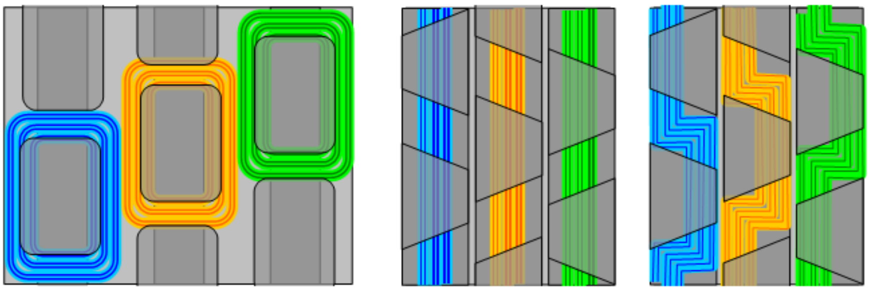

Figure 3.4 Left: Axially stacked three-phase winding with concentric coils in a radial flux machine. Middle: Solenoids axially stacked in a three-phase transversal flux machine. Right: Axially stacked three-phase wave-windings to form a combination of radial-to-transversal flux machine.

There are at least two winding configurations that can fulfil the primary winding specifications of high conductor fill factor and a compatible geometric shape for moulding. Both of these windings have the potential to be production-friendly. They are based on a circumferential distribution of coils or modular segments of coils and axially-stacked wave windings (see Figure 3.5).

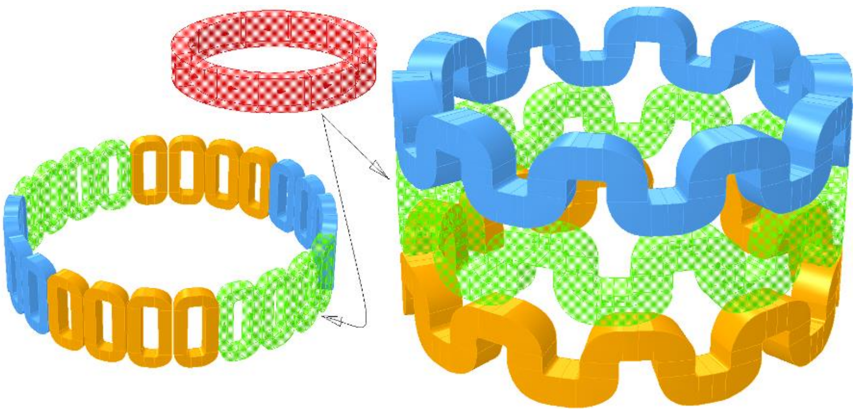

Figure 3.5 Left: Three-phase windings based on modular arrangements and circumferentially distributed coils. Right: Axially stacked three-phase wave winding.

Manufacturability plays a large part in the winding design for moulded machines, but there are other criteria that are at least as important, such as a good geometric design and a high fill factor in the winding. These criteria are mainly focused on the qualitative and quantitative aspects of the energy conversion in an electrical machine:

1) Torque capability (a quantitative aspect) is an outcome of the magnetic and electric loading in the machine. The torque capability is limited by the thermal loading in the machine.

2) Torque quality is at least as important as torque capability. This is an outcome of the magneto-mechanical alignments in the machine. Torque quality is expressed in terms of cogging and ripple.

3) Power conditioning of the machine, by specification of winding parameters such as number of winding turns, conductor area, and insulation which are related to speed, frequency, and terminal voltage in the machine.

Circumferentially distributed windings

Using the same number of rotor poles (N_p) and stator coils (N_s) will give a high torque capability, but the magneto-mechanical alignment will also give a high cogging torque. The cogging torque can be decreased by using a three-phase circumferentially distributed winding. The winding have N_s coils and rotor N_p poles, where the greatest common divisor between N_s

and N_p is close to 1. Practically speaking, this results in a winding arrangement with a number of coils that is $N_s = N_p \pm 1, \pm 2$ coils; see Figure 3.6. Where the coils are arranged in $N_s/3$ or $N_s/6$ respectively to divide the phase coils in one or two modules– modular windings [10].

Circumferential distribution of windings is thus a very useful configuration to have in moulded machines, especially when the number of poles and the cogging will be high. If used correctly, it can minimize cogging torque and simplify production when moulding a complete stator. The windings can be serially produced with good geometric tolerances, by being pressed to final shape in a fixture. For circumferentially distributed windings, the fixing of the winding is of special importance as the pole pitch is small. A minor misalignment when placing the winding in the mould is likely to have a major impact on the electric angle between the phases.

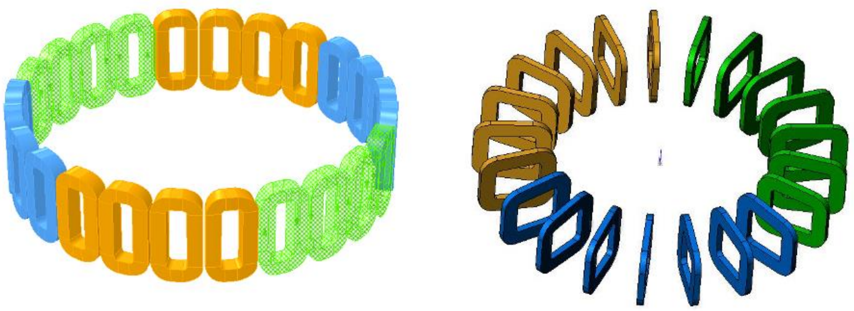

Figure 3.6 Three-phase windings based on modular arrangements and circumferentially distributed coils. Left: Two modules in each phase (represented by the same colouring). Right: One module in each phase.

Axially distributed windings

During moulding of a machine, the SM^2C material is a semi-floating mass; this can create problems in filling up all the spaces designed for the iron core in the winding. Wave winding seems to be one of the best winding types for dealing with this problem.

These windings are manufactured as a one-phase winding, and the machine is assembled by stacking three moulded winding segments axially (see Figure 3.5). These three winding segments are individually turned by 120º to create a three-phase winding. The segments are magnetically independent from each other, and each uses approximately 1/3 of the magnetization in the rotor.

The main advantage of this type of coil is the possibility to achieve simple winding production by pressing a basic circular coil to a wave winding; this gives a good chance of gaining a high repeatability in geometric tolerance. The challenge is to get the dimensions of the three different coils to such a standard that when the coils are axially stacked they will define the length of the stator during the moulding procedure in such a way that the voltage amplitude and the phase angle between the three phases do not differ from a symmetric split.

3.5 Summary

This chapter describes winding layouts in general, as well as the specific winding layouts that are suitable for moulding: circumferentially distributed windings and axially distributed windings. Wave winding seems to be especially interesting for axially distributed windings, which have the potential to be production-friendly with high fill factor and good geometric tolerances.

Chapter 4

Winding configuration experiments and moulding experience

This chapter describes a number of winding experiments and the experimental platform that was used. The experiments were performed to get a deeper understanding of winding design/configuration for machines moulded with SM^2C, and the impact of this on the performance of the moulded machine. The practical experience gained during these experiments and previous production of moulded machines is summarized below.

4.1 Background and test setup

The investigations of moulding electromagnetic circuits presented in this thesis started with two machines manufactured with SM^2C material and several different kinds of inductors. One of these machines was a claw-pole machine with a hoop coil, and the other was a torus-shaped machine with several independent coils connected together to create a three-phase winding. The windings for these two machines are simple to manufacture, and there are no direct problems in producing the two machines with good geometric outcome. The technical problems with the design and production of the windings started with a prototype production of a machine intended to pump cooling water for vehicle applications. The difficulty arose from the physical design of the winding, which was a type of circumferentially distributed winding; specifically, there were problems with producing this in a cost-effective way with good geometric tolerances.

Another SM^2C machine in a parallel project exhibited similar problems with the physical design and manufacturability of the windings, even though it had a completely different size and rotor construction. This started a series of discussions about windings and how to manufacture them. Even though the winding problem of the intended pump machine was solved to the extent of making it possible to create two working prototypes, it became evident that windings can create problems during moulding and will be a challenge for producing future machines.

A series of experiments was conducted to get a broad perspective of winding designs suitable for use in SM^2C machines. The focus of these experimental winding designs is to test a wide range of shapes and types of windings, and to evaluate their manufacturability and possibility of magnetic flux linkage. The different winding configurations are moulded in the existing mould from the previous production of the intended pump machine, since there is already a functional rotor and mould to use as a platform in the winding experiments. Table 4.1 presents the dimensions of the pump machine used as a platform, known as the P-machine.

Table 4.1 Dimensions of the P-machine

Rotor diameter	89 mm
Machine length	30 mm
Stator inner diameter	90 mm
Stator outer diameter	130 mm
Number of poles	22
Number of winding slots	21-24
Active magnet length	20 mm

The experiments are performed with 14 different moulded stators, including the two original designs, which worked as a reference for the tests. The electromagnetic force (EMF) was measured from each test, and the possibility of production of the windings is evaluated.

4.2 Winding experiments

The experiments are based on three winding concepts: I) three-phase circumferentially distributed windings, II) three-phase axially distributed windings, and III) one-phase windings. The main goal of the tests is to investigate the different winding configurations suitability for moulding and flux linkage, and a secondary goal is investigation of torque quality. In all of the tests, the windings were made by hand and moulded with the same 100-200µm iron powder except the first two ordinary prototypes of the pump machine, which used sorted and prepared iron powder. Figure 4.1 presents a small collage of pictures of the most interesting experiments, and Table 4.2 presents the stator (St) configurations and the results of the tests.

Figure 4.1 Three-phase windings based on modular arrangements and circumferentially distributed coils. Stator (St) configurations from top to bottom: St2, St4, St6, St9.

Table 4.2 Evaluation results of distributed concentrated winding (C), single-phase wave-winding (W), three-phase axially distributed wave-winding (WA) and three-phase circumferentially distributed wave-winding (WC)

	St1	St2	St3	St4	St5	St6	St7	St8	St9	St10	St11	St12	St13	St14
W-type	C	C	WC	W	WA	WA	WC	WC	WC	WC	WC	W	WC	WC
N-slots	24	24	24*	22	22	22	24*	24	24	21	21	22	21	21
N-turns/layers	3	3	3	1	1	1	1	1	1	1	2	2	3	3
N-module/group	2x3	2x3	1x3	1	1x3	1x3	1x3	2x3	2x3	1x3	1x3	1x3	1	1x3
W-diameter	0.2	0.2	0.8	0.8	0.8	0.8	0.8	0.8	0.8	0.8	0.8	0.8	0.8	0.8
N-strands	200	200	12	6	6	6	7	7	7	7	7	7	15	15
N-phases	3	3	3	1	3	3	3	3	3	3	3	1	3	3
E1, mVs	0.33	0.37	0.28 0.11	0.54	0.35 0.15	0.31	0.28		0.35	0.32	0.21	0.51	0.14	0.10
E2, mVs	0.36	0.36	0.27 0.11		0.11 0.27	0.15	0.33		0.34	0.31	0.20		0.12	0.09
E3, mVs	0.35	0.39	0.29 0.12		0.41 0.39	0.37	0.25		0.34	0.32	0.23		0.15	0.09
Ethd, %	0.4	0.1	0.2	0.3	0.8	0.8	0.2		0.2	0.7	0.3	0.0	0.1	0.1
shift 1, deg	0	0	0 6	0	0 183	0	0		0	0	0	0	0	0
shift 2, deg	117	115	-103 - 95		139 322	125	93		121	-126	-109		232	195
shift 3, deg	-121	-122	163 - 184		239 66	242	205		-115	230	119		92	43
Tcg, Nmm	100	110	100	60	70	40	30	10	30	30	60	60	40	50
Hs_{min}, mm	13	11	18	6	5	3	18	16	20	18	16	7	N	N
Hs_{max}, mm	18	17	24	8	8	4	22	18	22	19	18	9	N	N
Ws_{min}, mm	5	5	8	10	10	10	9	8	9	10	10	9	N	N
Ws_{max}, mm	6	7	12	13	12	12	11	10	11	12	12	11	N	N
Hw, mm	25	N	28	11	9-13	7-9	24	21	26	25	25	15	30	29
Hoff, mm	5±1	N	1.5	10	0	2	3±1	5	5	4	4	10	1	1
ΔH, mm	±1	N	±2	±1	±1	±0.5	±2	±1	±0.5	±1	±1	±1	±2	±2
Δθ, mm	±1	±2	N	±1.5	±1	±1	±3	±0.5	±0.5	±0.5	±1	±1.5	N	N

4.3 Moulding experience

When moulding a machine, there is a set of rules to follow and consider that will make the end result more predictable. This set of rules always starts with the geometric shape of the winding. In a conventional laminated machine, the iron core acts as a bobbin for the winding while at the same time defining the magnetic flux path. When moulding an electrical machine, the geometric form and placement of the winding define the structure of the iron core. Thus the geometric tolerances of the winding and the placement of the winding in the mould are of vital importance to the end result, as will be shown in the coming sections.

The fact that the winding determines the geometry of the iron core, and thus the flux path in the machine, can lead to several problems; these are described below.

Winding geometry

When making a winding intended to be moulded, the geometry of the winding is of significant importance to the end results. The winding is a bundle of conductors, and this makes it hard to control the winding geometry during production in such a way that it has a good fit in the mould during moulding. The winding usually becomes bigger than intended due to the springiness of the materials; if this is allowed to happen, it will decrease the space intended for the iron core and thereby decrease the power of the machine. When SM^2C is in a liquid state it will fill up every unintended gap in the winding, which may create shortcuts in the flux path.

Winding fixation

For repeatability, the winding needs to be fixed in a well-defined way. The SM^2C material is best utilized with high electric frequency, which means using a high number of poles in the machine. However, as the number of poles increases, the angular pole pitch becomes small, which in turn increases the physical tolerances of the winding. This means that if the three-phase winding is not aligned and fixed correctly, there will be a large difference in electric phase angle between the winding segments. If the machine is to function as required, it is of great importance to fix the winding with high precision. This can be achieved with different moulding techniques and machine layouts.

Winding connections

One of the more difficult aspects of moulding machines is the handling of winding connections during the moulding process. A three-phase winding will usually have six connections. Depending on the design of the winding, the thickness of the conductor, and the moulding method, the handling of the winding connections can be completely different from case to case.

Selection of moulding method

There are two basic rules for selecting the moulding method. First, if the machine is an outer rotor machine, then a radial rotocast technique is usually preferable. Second, if the machine is an inner rotor machine, then lateral linear moulding is a well-tested technique but carries the difficulty of handling the winding connections during moulding and thereby the requirements on surface smoothness of the moulded stator sides. There is a method using radial rotocast for an inner rotor machine that will give good surface requirements, but this needs to be tested further as it has only been used once.

4.4 Summary

The winding is a highly important aspect of moulded machines, and is the one thing that can influence the result of the moulding the most. The geometry and placement of the winding affects phase angles, size and tolerances of the mould, cogging torque, and the power rating of the moulded machine. It is thus recommended to start the design with a consideration of the winding, and to let the winding influence the rest of the machine design.

Chapter 5

Design and construction of a three-phase prototype generator

5.1 Motivation

The three-phase automobile generator is one of the most common types of generator. The automobile generator works at high electric frequency; this makes it an interesting application for the SM^2C material, since the material has low high-frequency losses. It is also possible that the SM^2C material could improve the performance of the machine.

5.2 Specification

The specification of the automobile generator used as a design goal in this chapter is given in Table 5.1.

Table 5.1 Specifications for an automobile generator

Power	3 KW
Working rotational speed	4000–14000 rpm
Number of phases	3
Rotor	Electric magnetized
Stator segments	Phases axially placed
Available stator length	80 mm
Rotor diameter	110 mm
Stator inner diameter	112 mm
Stator outer diameter	142 mm
Stator segment length	25 mm
DC voltage (after rectification)	28.8 V[1]
DC current	110 A

The reference generator is specified in Table 5.2.

Table 5.2 Specifications for the reference automobile generator

Power	3 KW
Working rotational speed	4000–14000 rpm
Number of phases	3
Number of poles	12
Rotor	Electric magnetized
Stator segments	Overlapping three-phase wave winding
Stator length	80 mm
Active length	36 mm
Rotor diameter	110 mm
Stator inner diameter	112 mm
Stator outer diameter	142 mm
Voltage (after rectification)	28.8 V[1]
DC current	110 A

In the reference generator, the physical length of the stator is 80 mm including the end turns, but the active length of the stator is only 36 mm. Thus there is a possibility to increase the usage of the existing stator length by moulding the stator in order to increase the active length.

5.3 Generator design

Since the stator is to be moulded, it is designed for a simplified production. In this context, the stator winding configuration is altered from a conventional complex three-phase stator to a stator made of three segments of a single phase in each segment. These segments are placed axially in the stator house, one after each other; see Figure 5.1. Similar designs have previously been used with SMC material [13][14]. The electromagnetic design simulates a single phase and is recalculated to correspond to a three-phase machine, as the phase output power times three is the total amount of output power from the three-phase machine.

Figure 5.1 Three stator segments stacked axially to create a three-phase stator.

The simulations are performed with the free program Finite Element Method Magnetics (FEMM) together with several MATLAB scripts to configure the machine dimensions, material properties, and electrical properties, to post-process the FEMM data, and to present the results. FEMM is a 2D simulation program (see Figure 5.2) which is chosen for its ability to give quick results and its compatibility with MATLAB. The major parts of the MATLAB scripts were developed by Avo Reinap, Dan Hagstedt, and Francisco Marques at the Division of Electrical Engineering and Automation, Lund University.

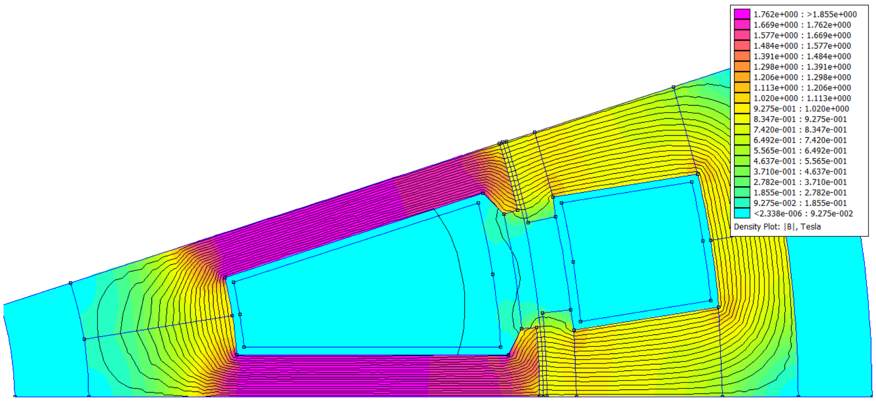

Figure 5.2 A plot from the Finite Element Method Magnetics (FEMM) program.

The use of MATLAB with FEMM allows one to make several iterations of simulations with different machine configurations such as material selections, number of poles, slot sizes, current settings, and rotor positions, all in a relatively short time span. It could be argued that it would be better to use a 3D simulation program to get a more exact representation of the machine, but this would be considerably more time consuming. Hence, in this part of the machine design, 2D simulations were preferred as the purpose is to determine winding and stator dimensions for the mechanical design of the machine.

Rotor configuration

The simulations described below used the default values for rotor configuration; there is no attempt at optimization of the rotor in this stage of the design.

Number of slots versus number of poles

The first three simulations are performed in pursuit of an initial rough design for the generator and to get an indication of how different relations between rotor pole and stator slot numbers can be used to optimize the electric design of the machine. It should be remembered that the magnetic coupling between rotor and stator will generally decrease with mismatch of poles and slots, but this mismatch also has the advantage of minimizing the cogging torque in the generator and thereby reducing generated sound.

The simulation is performed in three steps, with the number of stator slots differing from the number of rotor poles by -1, +1, and 0, respectively. The number of poles is varied from 8 to 24 in order to decide the pole range to be used in further simulations to investigate tooth tip design, rotor design, and to perform a full evaluation of the complete generator. In the simulations, the torque is calculated for one phase and at a fixed angle of 90 electrical degrees for the rotor/stator position, instead of varying the position to get an average value of the torque. This is done to minimize time consumption in the simulations while still getting a rough idea of the performance of the generator.

In Figures 5.3–5.5, the x-axis is the number of poles and the y-axis is the relative stator slot width, defined as:

$$K_s = \frac{slot\ width}{slot\ pitch}$$

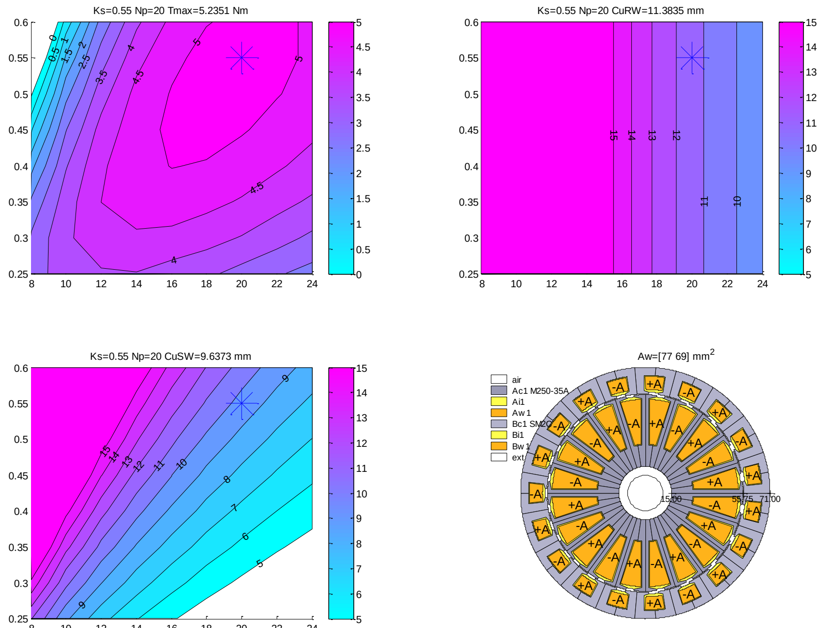

Figure 5.3 Simulation results for the generator with -1 stator slot relative to rotor pole number. Top left: the calculated torque for one phase. Top right: the rotor winding width. Bottom left: the stator winding width.

Bottom right: a representation of the machine configuration that gives the maximum torque.

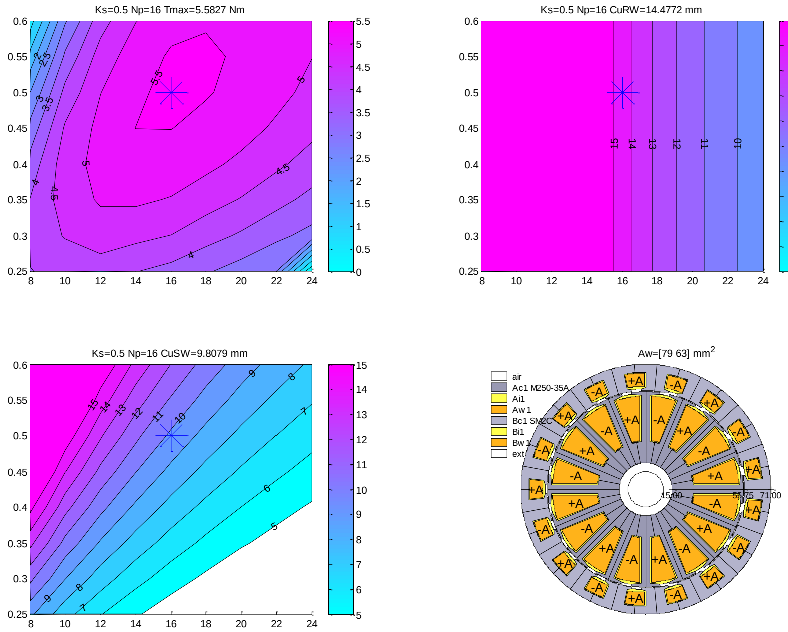

Figure 5.4 Simulation results for the generator with +1 stator slot relative to rotor pole number. Top left: the calculated torque for one phase. Top right: the rotor winding width. Bottom left: the stator winding width. Bottom right: a representation of the machine configuration that gives the maximum torque.

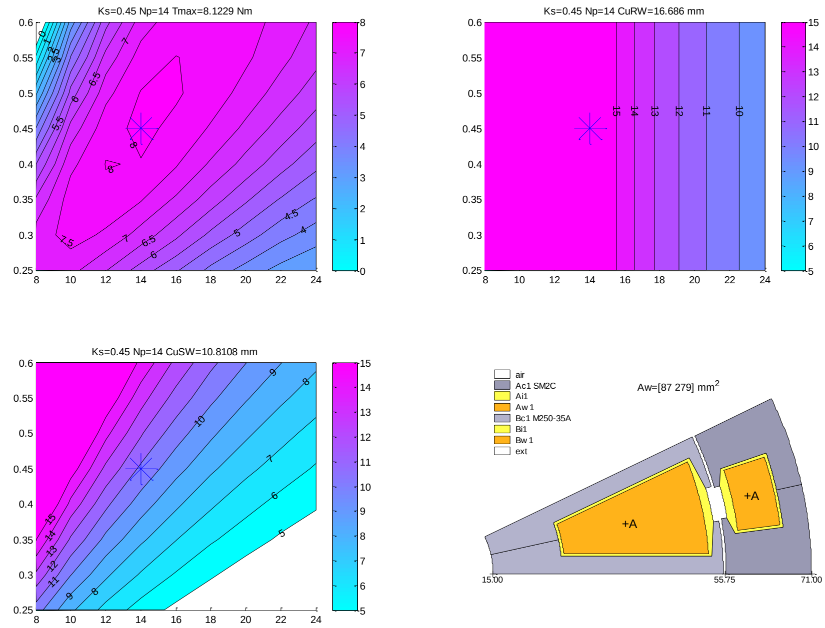

Figure 5.5 Simulation results for the generator with equal numbers of stator slots and rotor poles. Top left: the calculated torque for one phase. Top right: the rotor winding width. Bottom left: the stator winding width. Bottom right: a representation of the machine configuration that gives the maximum torque.

Table 5.3 A summary of the simulation results.

Number of stator slots compared to number of rotor poles	Max torque [Nm] for one phase	Winding width of the stator [mm]	Number of poles at max torque
-1	5.23	9.6	20
+1	5.58	9.8	16
Equal	8.12	10.8	14

These initial simulations showed that an equal number of slots and poles is to be preferred in the machine design, even though there is a possibility that this will increase the cogging torque and thus increase the noise produced by the machine when in operation. There is also the practical issue of the active length in the machine to consider. For lower numbers of poles, the end turn of the winding will be relatively large and will take up an increased amount of the length of the stator segment. This will decrease the active length, and in practice the machine will become a full claw pole machine instead of a semi claw pole machine. For this reason, the simulations described below used a pole range of 16–20 poles.

Tooth tip design

The tooth tip collects the magnetic flux which links with the stator winding. Simulations are performed to investigate how the tooth tip width affects the ability of the magnetic flux created in the rotor to link with the winding. The tooth tip width was varied in steps, in order to evaluate which width gives the highest torque and therefore the highest flux linkage. The tooth tip width is simulated with a current density of 7 A/mm^2 in the rotor and 12A/mm^2 in the stator. The relative tooth tip width is varied in steps from 0.9 down to 0.1 (see Figure 5.6), where a tooth tip width of 0 corresponds to straight teeth and a tooth tip width of 1 corresponds to no slot opening at all.

Table 5.4 Results of the simulations with varying relative tooth tip width.

Relative tooth tip width	Torque [Nm]
0.9	2.6320
0.8	2.7854
0.7	2.8739
0.6	2.9368
0.5	2.9766
0.4	3.0039
0.3	3.0111
0.2	2.9897
0.1	2.9664

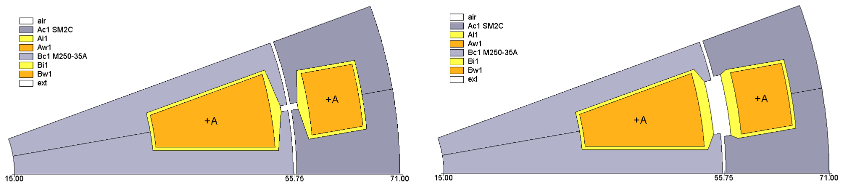

Figure 5.6 Left: relative tooth tip width of 0.9. Right: relative tooth tip width of 0.1.

As can be seen in Table 5.4, the torque values and thus the flux linkage remain similar when the tooth tip width varies between 0.5 and 0.1, with a maximum value at 0.3.

Rotor design

The rotor is intended to cover all three stator segments, and so each stator segment had 1/3 of the total rotor area. In the following simulations, the torque is calculated by sweeping the rotor from $\pi/2$ to $-\pi/2$ in steps of $\pi/30$, and then calculating an average value of the torque. The torque is calculated for one phase. The relative radial rotor slot length measured from the centre of the rotor axes (K_y) is set to 0.4, 0.5, and 0.6, in combination with relative rotor slot widths (K_s) of 0.35, 0.45, and 0.55, respectively. The number of poles varied from 14 to 22 and the stator slot width varied from 0.25 to 0.60 in steps of 0.05. The simulations are presented in order from Figure 5.7 to Figure 5.9.

Set of rotor design parameters: $K_y = 0.4$, $K_s = 0.35$

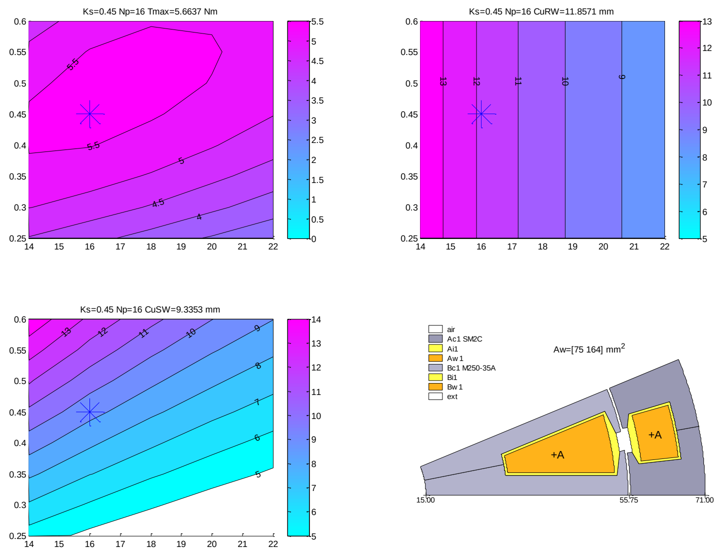

Figure 5.7 Simulations with K_y = 0.4 and K_s = 0.35. Top left: simulated torque. Top right: rotor winding width in mm. Bottom left: stator winding width in mm. Bottom right: machine diagram. The y-axes show relative stator slot width and the x-axes show the number of poles.

Set of rotor design parameters: K_y = 0.5, K_s = 0.45

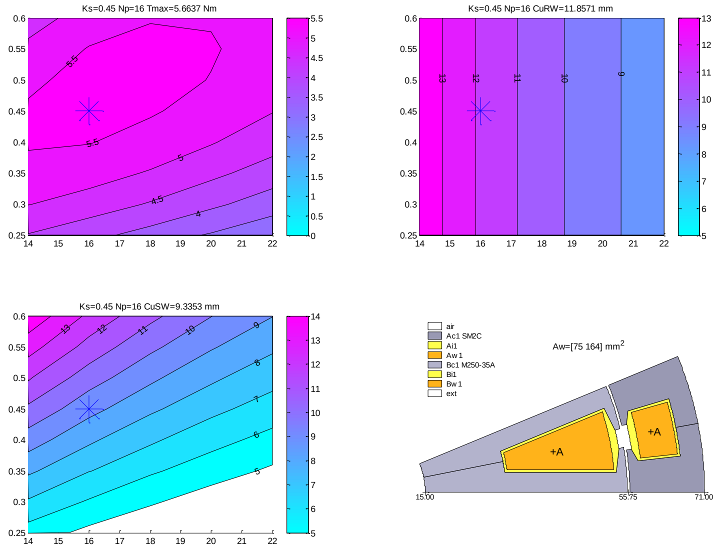

Figure 5.8 Simulations with K_y = 0.5 and K_s = 0.45. Top left: simulated torque. Top right: rotor winding width in mm. Bottom left: stator winding width in mm. Bottom right: machine diagram. The y-axes show relative stator slot width and the x-axes show the number of poles.

Set of rotor design parameters: K_y = 0.6, K_s = 0.55

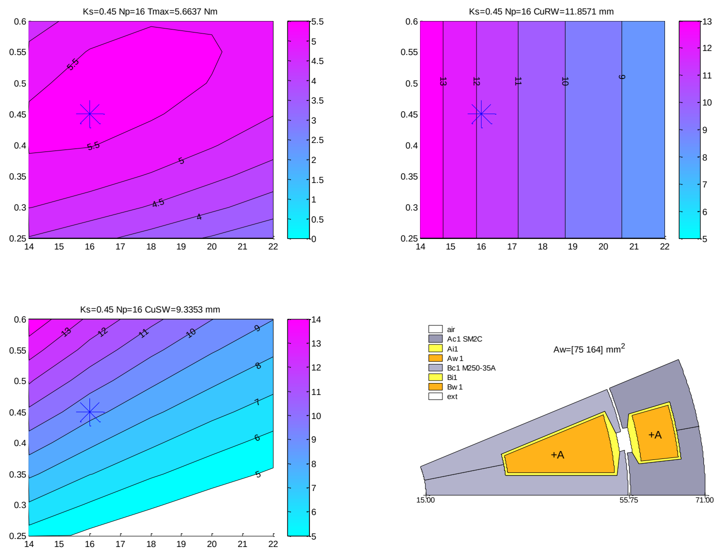

Figure 5.9 Simulations with K_y = 0.6 and K_s = 0.55. Top left: simulated torque. Top right: rotor winding width in mm. Bottom left: stator winding width in mm. Bottom right: machine diagram. The y-axes show relative stator slot width and the x-axes show the number of poles.

Summary of the simulation results:

- The rotor configuration with K_y = 0.4 and K_s = 0.35 gives a maximum phase torque of 5.6637 Nm with 16 poles and a stator slot relative angular width of 0.45. The coil width at maximum torque is 11.9 mm.

- The rotor configuration with K_y = 0.5 and K_s = 0.45 gives a maximum phase torque of 5.5231 Nm with 18 poles and a stator slot relative angular width of 0.5. The coil width at maximum torque is 10.7 mm.

- The rotor configuration with K_y = 0.6 and K_s = 0.55 gives a maximum phase torque of 5.0924 Nm with 18 poles and a stator slot relative angular width of 0.5. The coil width at maximum torque is

11.3 mm.

The following simulations used a pole range of 16 to 20 poles. Selection of a rotor configuration is a combination of torque and the size of the rotor winding. Since the available space in the machine is limited, the rotor winding size has a considerable influence on the decision. The rotor configuration used in the simulations is K_y = 0.5 and K_s = 0.45, and the conductor fill factor is assumed to be 0.7.

Generator performance simulations

In order to investigate copper losses, torque, efficiency and temperature at continuous operation, a fixed current density in the stator is assumed. The current density in a stator segment is calculated from the intended maximum current output from the complete generator and the conducting area of the copper wire that is suggested for the stator segment winding in the generator. In these simulations, a square copper wire with a 2 x 2 mm cross-section is chosen, giving an increased chance for a conductor fill factor of 0.7 in the slot. The generator is assumed to have a rectified output voltage of 28.8V and a maximum rectified current of 110 A. The generator is delta connected, and so the peak current density in a stator segment winding is given by:

$$\hat{i}_w = \frac{110}{\sqrt{3}} = 63.5A$$

$$\hat{j}_{cd} = \frac{\hat{i}_w}{A_{cu}} = \frac{63.5}{4} = 15.875A/mm^2$$

In the generator performance simulations, the stator segment peak current density is fixed at 16 A/mm^2 with a fill factor of 0.7. The tangential stator coil width is changed from 0.40 to 0.70, where 0.40 is the narrowest coil width and 0.70 is the widest coil width. The current density in the rotor varied from 5 A/mm^2 to 15 A/mm^2 with a fill factor coefficient of 0.7.

The results of the simulations are presented in Figure 5.10–Figure 5.12 and summarized in Table 5.5.

Simulation results with 16 poles

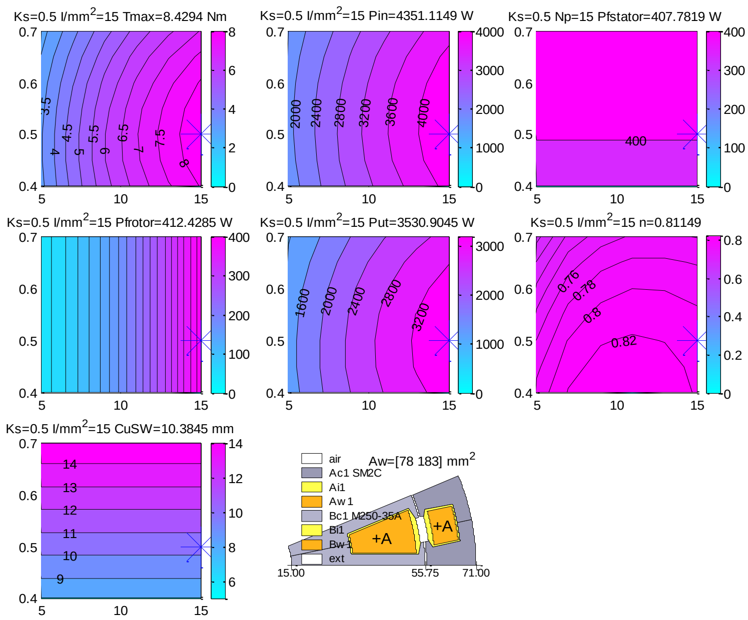

Figure 5.10 From top left to bottom right: torque, power in, power loss in stator, power loss in rotor, power out, efficiency, stator segment winding width, and machine diagram. The x-axes correspond to the rotor current density and the y-axes correspond to the stator slot width.

Simulation results with 18 poles

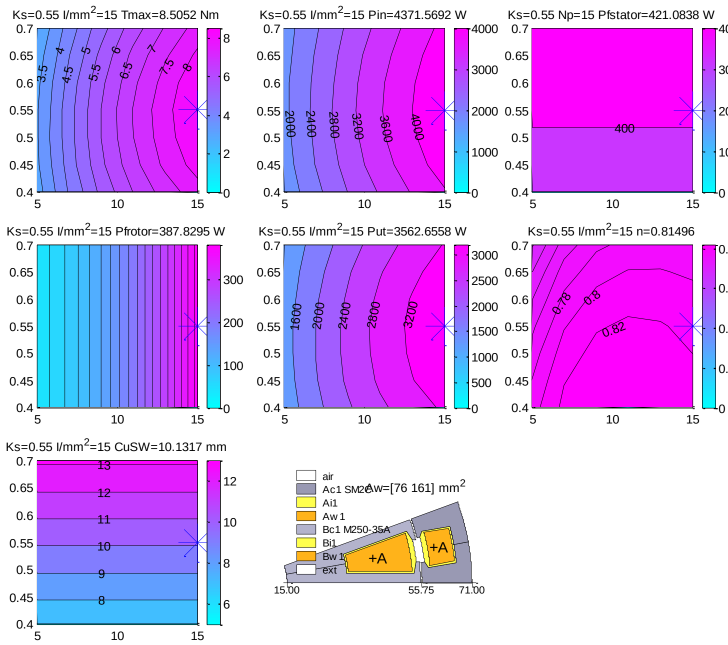

Figure 5.11 From top left to bottom right: torque, power in, power loss in stator, power loss in rotor, power out, efficiency, stator segment winding width, and machine diagram. The x-axes correspond to the rotor current density and the y-axes correspond to the stator slot width.

Simulation results with 20 poles

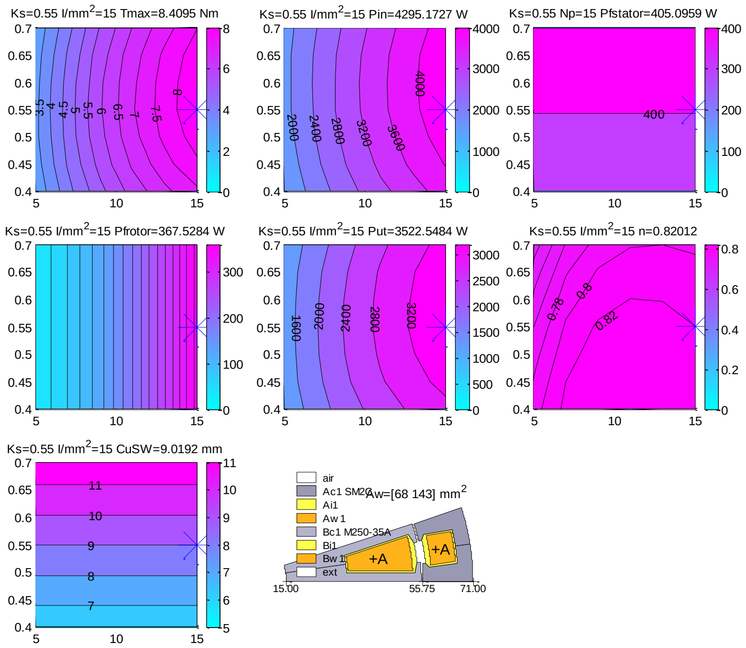

Figure 5.12 From top left to bottom right: torque, power in, power loss in stator, power loss in rotor, power out, efficiency, stator segment winding width, and machine diagram. The x-axes correspond to the rotor current density and the y-axes correspond to the stator slot width.

Table 5.5 Simulation results using 16-20 poles

Number of poles	16	18	20
Torque (max)	8.4294 Nm	8.51 Nm	8.41 Nm
Stator Pcu	407.8 W	421.1 W	405.1 W
Rotor Pcu	412.5 W	387.8 W	367.5 W
Efficiency	0.812	0.815	0.82
Coil width	10.4 mm	10.1 mm	9.0 mm
Pout	3530.9 W	3562.7 W	3522.5 W

The three designs appear to be almost equal in torque performance and in efficiency. The stator coil width in these simulations is 10.4 mm for 16 poles, 10.1 mm for 18 poles, and 9 mm for 20 poles. As shown in Table 5.5, the 18-pole design has a slight advantage in torque and thus also in output power, but the 20-pole design has the highest efficiency and lowest losses, especially in the rotor, where heat removal is more difficult.

5.4 Thermal calculations

Thermal calculations of the steady state temperature in the designed moulded generators are based on a simulated temperature study of the conventional automotive generator with 12 poles at steady state (Figure 5.13). The existing 12-pole generator has a specific cooling capability, and the expectation of the new generator is that it will be able to handle the same temperature rise as the existing 12-pole generator. This was investigated by examining the steady state temperature of the existing 12-pole generator with natural convection is used for cooling, and then comparing the information from this simulation with the simulations of the three models of the new generator with 16, 18, and 20 poles.

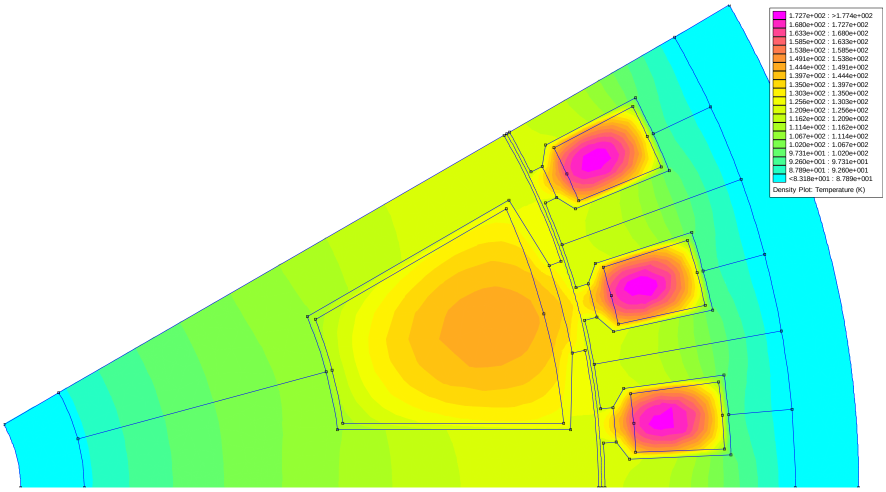

Figure 5.13 Heat simulation in the existing 12-pole generator.

The heat simulation of the existing 12-pole automobile generator use a rotor current density of 7 A/mm^2, a stator current density of 25 A/mm^2, and a fill factor of 0.5 in the stator and rotor. A FEMM program is used to simulate the thermal steady state in the design of the generators. The simulation results suggest that the heat radiation from this generator will have a value of 800 W/(m^2*°K) given a surrounding air temperature of

70 ºC. This corresponds to a surface power dissipation from the stator yoke of 13947W/m^2. The hot spot in the stator coil is 176 ºC and the hot spot in the rotor is 147.5 ºC. This may seem quite high, but if it is possible to cool down the 12-pole generator it should be possible to cool down the new design if it has similar temperature values.

The thermal simulations of the 16, 18, and 20 pole generators use a rotor current density of 11 A/mm^2 and a stator current density of 16 A/mm^2 (see Figure 5.14–Figure 5.16). The heat radiation from the stator yoke is set to 800 W/(m^2*ºK), in line with the results from the 12-pole generator. With a surrounding air temperature of 70 ºC, the hot spots in the stator coils were as given in Table 5.6.

Thermal simulation results with 16 poles

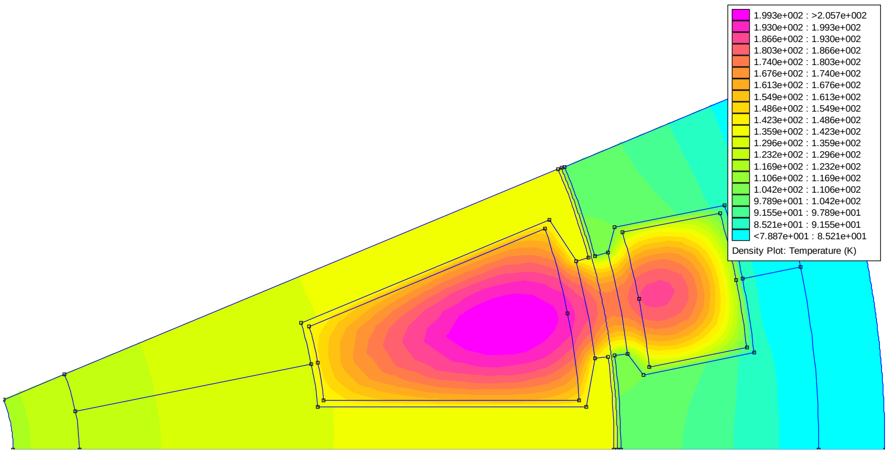

Figure 5.14 Thermal simulation in the 16-pole generator with a surrounding air temperature of 70 ºC and the thermal radiation from the stator yoke set to 800 W/(m2*ºK). The hot spot in the stator coil is 188 ºC and the hot spot in the rotor is 205 ºC.

Thermal simulation results with 18 poles

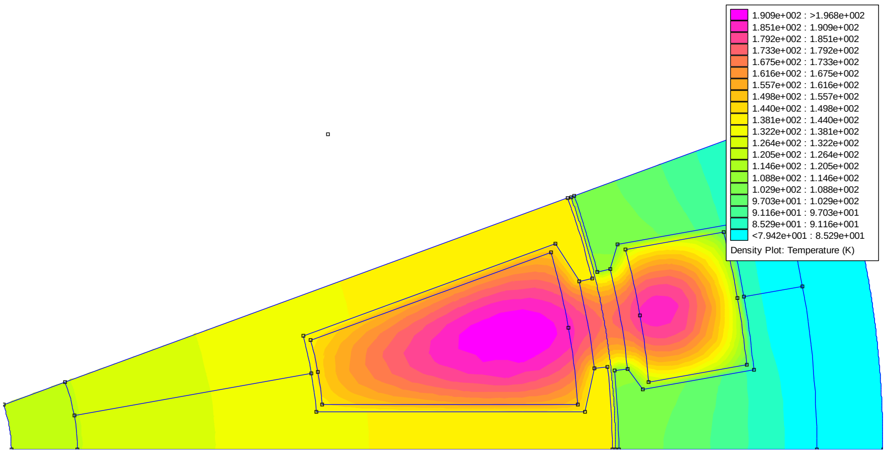

Figure 5.15 Thermal simulation in the 18-pole generator with a surrounding air temperature of 70 ºC and the thermal radiation from the stator yoke set to 800 W/(m^2*ºK). The hot spot in the stator segment coil is 188 ºC and the hot spot in the rotor is 196 ºC.

Thermal simulation results with 20 poles

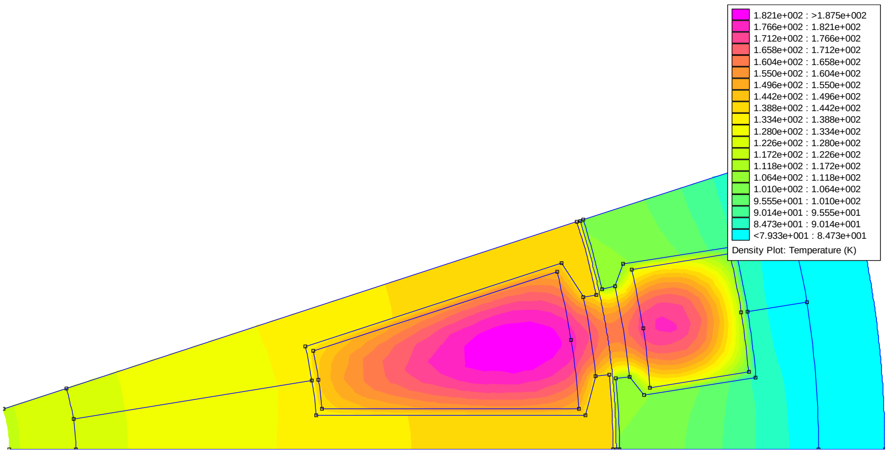

Figure 5.16 Thermal simulation in the 20-pole generator with a surrounding air temperature of 70 ºC and the thermal radiation from the stator yoke set to 800 W/(m^2*ºK). The hot spot in the stator coil is 177 ºC and the hot spot in the rotor is 187 ºC.

In all three thermal simulations, the hotspot in the rotor is larger than the hotspot in the stator segments. This could be considered a problem, as it is usually more difficult to remove heat from the rotor due to the air gap between rotor and stator. Although these thermal simulations do not represent the whole truth, they still give helpful guidance regarding the important aspect of how to cool the generator.

Table 5.6 Results from thermal simulations

Design	16 poles	18 poles	20 poles
Torque (Nm)	7.2	7.2	7.2
Pout (W)	3000	3000	3000
Efficiency	0.812	0.815	0.82
Hot spot S (˚C)	189	188	177
Hot spot R (˚C)	205	196	187

5.5 Summary of the design

Table 5.7 summarizes the simulated performance of the designed SM^2C generator in comparison with the original/reference generator.

Table 5.7 Design comparisons of designed and reference generator

	Reference generator	Designed generator	Unit
Total length, including end windings	0.08	0.08	[m]
Active length	0.036	0.053	[m]
Stator outer diameter	0.142	0.142	[m]
Air gap length	0.0005	0.0005	[m]
Rotor base speed	4000	4000	[rpm]
Rotor max speed	14000	14000[1]	[rpm]
# poles	12	20	
Air gap flux	0.58	0.40	[T @ RMS]

density @ no load			
Current density stator (3000W)	25	16	[A/mm^2]
Current density rotor base speed	7	11	[A/mm^2]
Current density rotor nominal speed (7500 resp 10000 rpm)	3	5.5	[A/mm^2]
Current density rotor max speed	1.5	2.8	[A/mm^2]
Base electric frequency	300	667	[Hz]
Max electric frequency	1400	2333[1]	[Hz]
Stator copper losses at base speed	800	405	[W]
Stator iron losses at base speed	200	15	[W]
Rotor copper losses at base speed	140	197	[W]
Rotor iron losses at base speed	170[2]	50[2]	[W]
Max torque at base speed	9.55	7.2	[Nm]
Max torque at nominal speed	4	3.5	[Nm]
Max torque at max speed	2	1.8	[Nm]
Max power at base speed	3000	3000	[W]
Efficiency at max power at base speed	0.68	0.79	
Efficiency at max	0.68	0.85[3]	

power at nominal speed			

1. This limitation does not consider mechanical stress in rotor structure due to the high rotation speed.
2. Rough estimation of tooth tip losses in rotor.
3. Rough estimation of efficiency due to decreased DC losses in rotor.

5.6 Building the prototype stator

The production of the stator prototype began with production of the winding. The most difficult part of this was to design the stator winding for manufacturability. Three different windings are manufactured; two of them handmade, and one produced within a fixture by pressing the copper wire to its designed shape.

Windings

The first winding is handmade from a round copper conductor with a diameter of 2.3 mm and 15.5 turns. The particular difficulty with making the handmade prototype winding lay in the approach of bending the whole wire into a pattern that would upon being wound up create the winding (see Figure 5.17). This bending can be done by machine, and so it is not particularly difficult to produce this kind of winding as there are a number of wire bending machines available today.

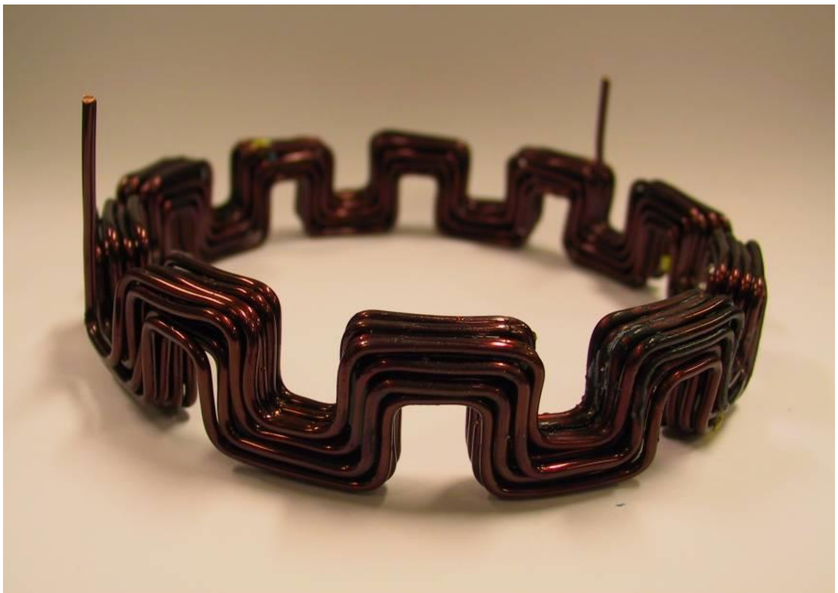

Figure 5.17 A handmade winding with a round conductor and 15.5 turns for the first stator segment.

The second winding is very similar to the first winding, the main difference being that instead of a round conductor with 15.5 turns, it is constructed from a rectangular conductor with dimensions 1.5 x 3.2 mm and 18 turns (see Figure 5.18). The intention behind using this kind of conductor in the winding is to maximize the conductor fill factor in the slot of the stator.

Figure 5.18 A handmade winding with a square conductor (to increase the copper fill factor) and 18 turns.

The third winding is manufactured in a fixture by pressing a hoop coil into a wave winding. This conductor has the same dimensions and the same number of turns as the second winding. The main difference is the shape of the winding; this winding is pressed to a sinusoidal shape (see Figure 5.19). The pressing caused some damage to the winding insulation, especially in the corners of the slots.

Figure 5.19 A fixture-pressed sinusoidal wave winding with 18 turns.

There are some differences between these three windings. Using a rectangular wire instead of a round wire increases the copper fill factor in the winding, and thereby decreases the losses depending on the current in the winding. The fixture-pressed third winding is probably the easiest to produce in mass production, but since it does not have the desired geometric rectangular shape there is a significant risk that the flux linkage will be decreased and the machine will not be able to produce the required output power. There is also a significant risk that the fixture-pressing process will damage the insulation and the conductors in the winding layer closest to the press fixture.

Moulding of segments

The mould consists of two parts. The first is a central piece (see Figure 5.20) to define the air gap between rotor and stator and create the moulded teeth in the stator. The second part of the mould defines the outer diameter of the segment and the 120º phase difference between the stator segments. This mould does not include a lid to define the upper side of the segment, due to the geometric differences in winding length between the prototype windings. The material in the mould is POM-C; this is a plastic that is easy to work with and very hard to glue, making it suitable for a prototype mould for the segments. The downside of POM-C as a mould material is its large thermal expansion.

Two moulded segments are produced with windings 1 and 3, using gravitational moulding and an iron powder with a particle size of 100-200 µm. The epoxy used in the moulding is Araldit LY 5052 mixed with Aradur 5052. The iron powder is heated to 65ºC to make the mixture more viscose and facilitate the moulding. The mixture is injected into the mould, and the mould is placed in an oven at 60ºC in order to decrease the time taken for the mixture to cure and develop a solid state. The material classification from the moulding is SM^2C-G.

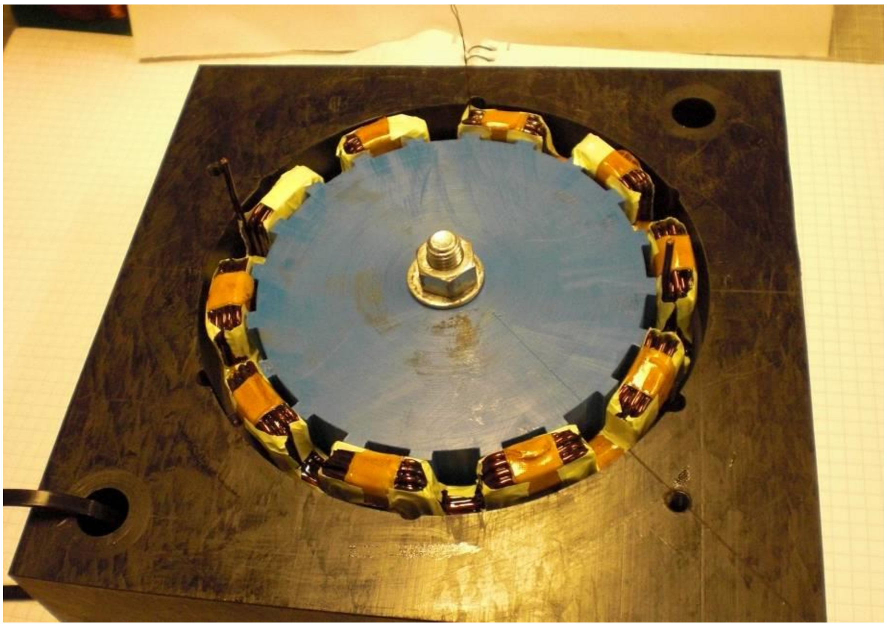

Figure 5.20 The mould with stator winding 1 placed in it just before moulding.

5.7 Building the prototype rotor

The rotor constructed for the prototype is a compromise between the intended full-length rotor and a rotor with decreased length which allowed testing of the different segments separately. The rotor is limited in active length to one segment length, and is made of four parts: an axis, two semi claw-pole structures, and a winding for magnetization of the rotor. The material in the rotor core is a weldable material equivalent to Swedish standard steel 1672. The two semi claw-pole structures are based on a solid round core with milled slots for the correct positioning of the teeth, and the teeth are welded into the slots (see Figure 5.21). Four screws are used to assemble the rotor, making it possible to quickly assemble and disassemble the rotor as required.

The dimensions of the rotor core are based on the FEMM calculations described earlier in this chapter; see diagrams in appendix A.

Figure 5.21 The prototype rotor, disassembled.

The rotor core is magnetized using a winding made of 8 turns of a spun wire consisting of 7 parallel conductors, each with a diameter of 0.8 mm. The conductors in the spun wire are series-connected to form a winding with 56 turns. This give the rotor a copper fill factor of 0.218, which is low compared to the simulated value but is considered sufficient for the testing of the different moulded stators. Figure 5.22 shows the assembled rotor together with a stator segment.

Figure 5.22 The prototype rotor assembled together with a stator segment.

5.8 Summary

This chapter describes the electromagnetic design of the intended automobile generator and a thermal investigation of the same. The top three generator configurations showed almost equal behaviour in the simulations, but the thermal load was lowest in the 20-pole generator. The chapter also describes the production of the prototype with three different stator windings and an electrically magnetized rotor.

Chapter 6
Generator measurements

This chapter presents the measurement results from the two prototype generator segments, including several different tests with dummy windings. Dummy windings are particularly useful in measuring flux linkage and flux leakage in a moulded segment, to get a deeper understanding of the design without building a full machine. This chapter also includes a discussion of the results and further analyses.

6.1 The test bench

During the production of the prototype generator, several tests of the electromagnetic coupling between rotor and stator are performed using dummy windings (see Figure 6.1). The electromagnetic coupling is measured by the EMF in the test coils. The tests used a machine housing and an electric magnetized rotor. To create the rotor excitation speed, a handheld drilling tool with two different rotation speeds is used to run the rotor.

The dummy windings are made in plastic with a 3D printer, with two EMF pickup test coils attached: one on the inside of the dummy winding close to the air gap to measure incoming flux in the segment, and the second on the outside of the dummy winding next to the yoke to measure the flux passing through the yoke. These test coils are used to measure the amount of flux leakage through the winding in a segment.

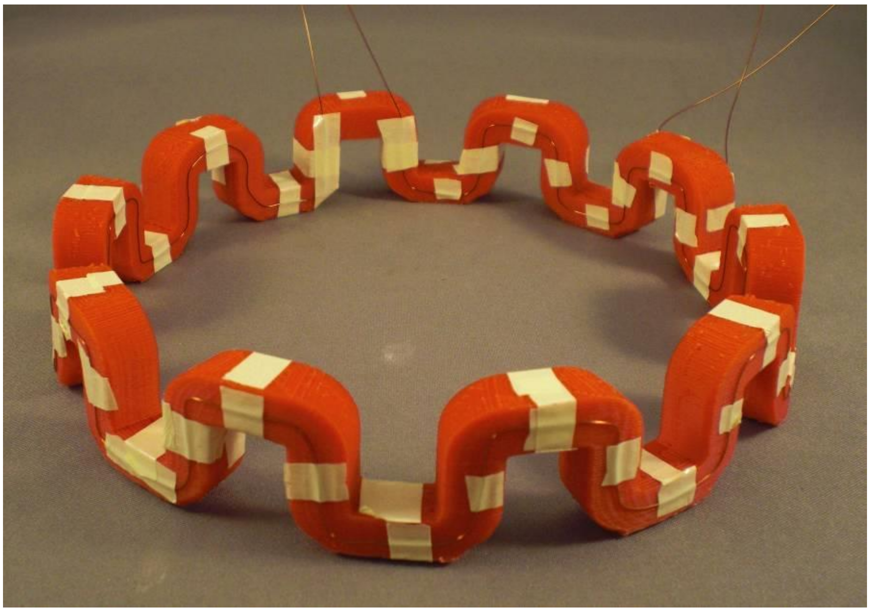

Figure 6.1 The 3D-printed dummy winding with two EMF pickup test coils, one on the inside and one on the outside.

In the power conversion tests of the two finished stator segments, a direct current machine capable of 4000 rpm and 500 W is used to create the excitation speeds, and two parallel-connected variable resistors are used as variable load. Two separate voltage supplies are used to apply magnetizing current in the DC machine and in the rotor of the generator. Multimeters are used to measure the voltage and current from the generator (see Figure 6.2).

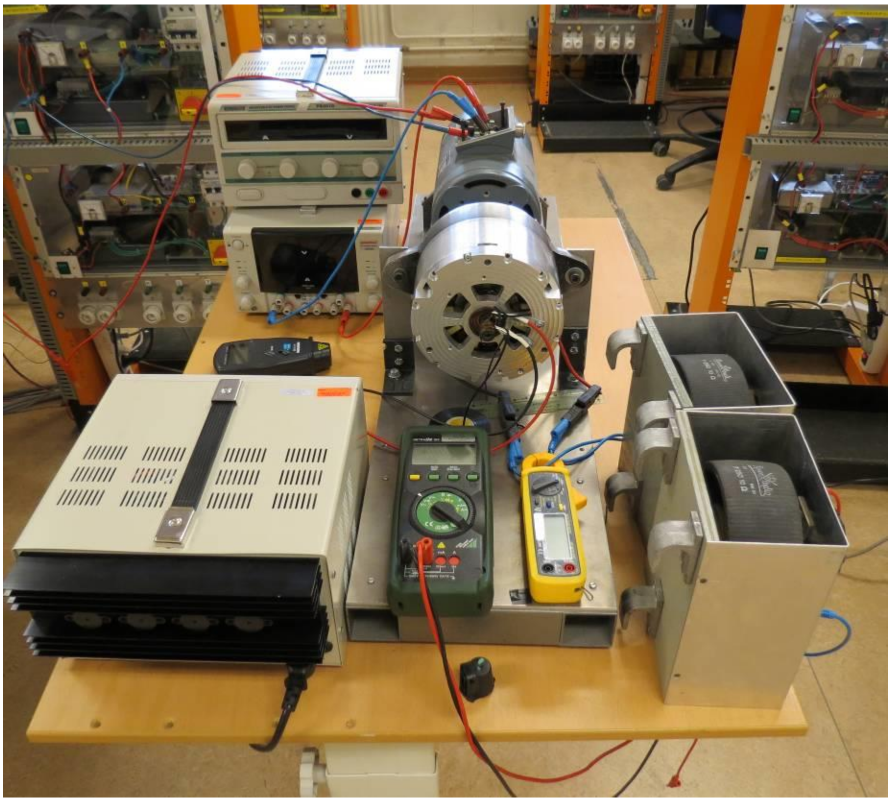

Figure 6.2 Setup for power conversion tests of the generator.

6.2 Electromagnetic measurements

During the tests, the focus is on two major goals:

1. To find a winding design with good electromagnetic properties suitable for production.

2. To investigate the impact of different SM^2C materials on the finished stator.

The dummy windings provided a fast way to elicit comparable test results for evaluation of material configurations, as the EMF test coils on these windings allows measurement of the induced voltage and thus calculation of the flux linkage.

The dummy winding tests are listed below, and described further in appendix C.

1. Moulded core of powder size 100-200 µm and epoxy NM FW 3070 mixed with NM 150B (ST1)

2. Moulded core of powder size 100-200 µm and epoxy Araldit LY 5052 mixed with Aradur 5052 (ST2)

3. Moulded core of “sorted and prepared” powder and epoxy Araldit LY 5052 mixed with Aradur 5052 (ST4)

4. Moulded core halves (Figure 6.4) of powder size 100-200 µm and epoxy Araldit LY 5052 mixed with Aradur 5052 (ST5)

Table 6.1 Data from tests with dummy windings, where the colours is to mark the change in excitation current used with each moulded dummy winding.

Case	Ψ_{m1}, [mVs]	Ψ_{rms}, [mVs]	E_{m1}, [mV]	E_{rms}, [mV]	Freq, [Hz]	I_{field}, [A]	U_{field}, [V]
ST1-LS-LC inner coil	0.16	0.12	0.16	0.11	67.2	4.01	7.5
ST1-LS-LC outer coil	0.10	0.07	0.10	0.07	67.2		
ST1-HS-LC inner coil	0.16	0.11	0.16	0.11	220.8	4.05	7.5
ST1-HS-LC outer coil	0.10	0.07	0.09	0.07	220.8		
ST1-LS-HC inner coil	0.30	0.21	0.28	0.21	68.8	7.96	15.0
ST1-LS-HC outer coil	0.18	0.13	0.17	0.12	68.8		
ST1-HS-HC inner coil	0.30	0.21	0.27	0.20	222.2	7.90	15.0
ST1-HS-HC outer coil	0.18	0.12	0.16	0.12	222.2		
ST2-LS-LC inner coil	0.21	0.14	0.19	0.14	68.2	4.02	7.5
ST2-LS-LC outer coil	0.13	0.09	0.12	0.09	68.2		
ST2-HS-LC inner coil	0.20	0.14	0.18	0.14	220.3	4.02	7.5
ST2-HS-LC outer coil	0.13	0.09	0.11	0.09	220.3		

ST2-LS-HC inner coil	0.39	0.27	0.33	0.27	68.1	7.93	14.9
ST2-LS-HC outer coil	0.24	0.17	0.21	0.17	68.1		
ST2-HS-HC inner	0.38	0.26	0.32	0.26	216.0	7.94	14.9
ST2-HS-HC outer coil	0.24	0.17	0.20	0.17	216.0		
ST4-LS-LC inner coil	0.24	0.17	0.20	0.17	67.4	4.68	7.5
ST4-LS-LC outer coil	0.14	0.10	0.12	0.10	67.4		
ST4-HS-LC inner	0.23	0.16	0.19	0.16	214.6	4.07	7.5
ST4-HS-LC outer coil	0.13	0.09	0.11	0.09	214.6		
ST4-LS-HC inner	0.42	0.30	0.33	0.29	67.1	7.85	14.9
ST4-LS-HC outer coil	0.24	0.17	0.19	0.17	67.1		
ST4-HS-HC inner	0.43	0.30	0.33	0.30	209.6	7.90	14.9
ST4-HS-HC outer coil	0.24	0.17	0.18	0.17	209.6		
ST5-LS-LC inner	0.15	0.10	0.14	0.10	67.1	4.05	7.5
ST5-LS-LC outer coil	0.10	0.07	0.10	0.07	67.1		
ST5-HS-LC inner	0.14	0.10	0.14	0.10	213.2	4.12	7.5
ST5-HS-LC outer coil	0.10	0.07	0.10	0.07	213.2		
ST5-LS-HC inner coil	0.27	0.19	0.26	0.19	68.6	8.00	15.0
ST5-LS-HC outer coil	0.19	0.13	0.19	0.13	68.6		
ST5-HS-HC inner	0.26	0.18	0.26	0.18	213.7	7.96	15.0
ST5-HS-HC outer coil	0.19	0.13	0.18	0.13	213.7		

The measurements made with the moulded dummy windings are comparable to the two real moulded stator windings if they are converted to the right winding turns for the two segments. Flux linkage values for a real winding will usually lie between the values for the inner and the outer EMF pickup coils in the dummy windings. The following observations can be made regarding the tests:

1. The moulding process and the quality of the binder have a remarkable influence on the magnetic characteristics of the core. This means that even if the moulding process is the same during every moulding, the results from each moulding can be different; the outcome is not predictable. The binder has two functions. The first is to ensure that the iron powder mixed in a liquid state reaches the intended area during filling of the mould. Second, after the fill, the non-essential binder should separate from the iron powder as the iron powder compresses (see Figure 6.3). If this does not occur, there will be a lower iron fill factor in the moulded segment. The first of these functions can create problems during the moulding process, which makes it hard to predict the outcome of each separate moulding. This problem results in a lower iron fill factor at local places in the moulded part, and can in some cases only be discovered by cutting through and thereby destroying it. Problems with the second function are easier to discover, as there will be no visible separation between iron powder and binder.

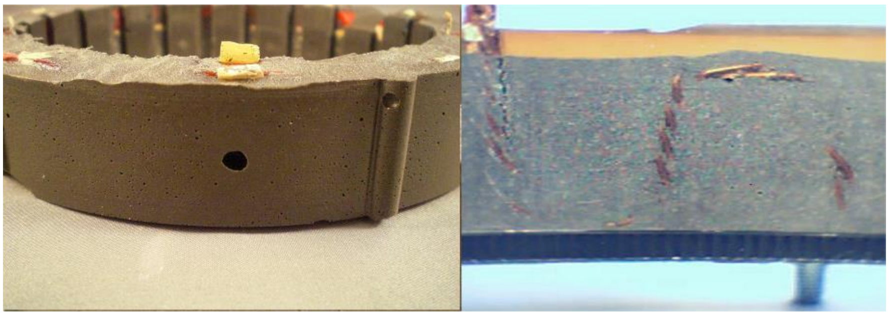

Figure 6.3 Left: Incomplete separation of excess binder from the iron core. The non-essential binder is still mixed with the iron powder. Right: Proper separation of excess binder from the iron core. The clear/yellowish layer at the top is the separated binder.

2. The difference in flux linkage between the powder of size 100-200 μm and “sorted and prepared” powder is relatively small, and is more noticeable in the inner test coil in the dummy winding (close to the air gap) than in the outer test coil (close to the yoke of the

stator).

3. In comparison to the stator moulded as a single piece, the stator made of two halves of SM^2C (Figure 6.4) showed a smaller difference between the near and far sensor coils and also considerably lower values in the near coil. This could be due to the moulding and the additional small air gap between the two halves in the yoke of the stator.

Figure 6.4 One of the two moulded core halves.

Further electromagnetic tests were performed with the completed stator segments, as described below.

Segment 1 included a handmade winding with 15.5 turns of a 2.3 mm diameter round conductor (Figure 5.17). The moulded segment has a measured resistance (with four terminal sensing) of R = 0.052 Ω,. The inductance of the segment are measured with an LCR-meter at 120 Hz and 1000 Hz. Table 6.2 gives a comparison of the measured inductance with calculated inductance from measurements of open circuit EMF and short-circuit current. The inductance is calculated with the equation

$$L = \frac{\sqrt{\left(\frac{U^2{}_{OC}}{I^2{}_{SCC}} - R_S^2\right)}}{2\pi f} \tag{1}$$

Table 6.2 Measured and calculated inductance from tests with segment 1. R = measured with rotor, UR = measured without rotor.

Case	L[mH]	X_s [Ω]	Freq, [Hz]	I_{field}, [A]	U_{field}, [V]
Measured-R	0.178	-	120	-	-
Measured-R	0.1674	-	1000	-	-
Measured-UR	0.163	-	120	-	-
Measured-UR	0.1623	-	1000	-	-
Calculated	0.1910	0.4000	333	10.0	6.36
Calculated	0.1839	0.4814	416.67	10.0	7.88
Calculated	0.1786	0.5612	500	10.0	9.26
Calculated	0.1709	0.6265	583.3	10.0	10.4
Calculated	0.1676	0.7019	666	10.0	11.7

Segment 2 included a pressed winding made in a fixture for repeated production, giving the winding good geometric tolerances (see Figure 5.19). This winding has 18 turns and use a square conductor in order to maximize the conducting fill factor in the winding. The winding have a resistance of 0.042 Ω. Table 6.3 presents measured and calculated inductance with the same methods as in segment 1. Due to its small active length, the winding has a sinusoidal geometric form from the compression in the fixture; this could be avoided with an increased active length.

Table 6.3 Measured and calculated inductance from tests with segment 2. R = measured with rotor, UR = measured without rotor.

Case	L[mH]	X_s [Ω]	Freq, [Hz]	I_{field}, [A]	$U_{no.load}$, [V]
Measured-R	0.2510	-	120	-	-
Measured-R	0.2425	-	1000	-	-

Measured-UR	0.198	-	120	-	-
Measured-UR	0.1976	-	1000	-	-
Calculated	0.2069	0.4334	333	10.0	4.52
Calculated	0.2028	0.6370	500	10.0	6.51

Further tests are performed with an excitation speed of 1000-2500 rpm and a rotor magnetizing current of 2-10 [A]. The rotor has 56 turns in its winding, giving a magneto motive force of 112-560 [A_{turns}] during the tests. The intended operating speed for the generator is 4000-14000 rpm, and the measurements are recalculated to match this. The flux linkage in the two stator segments is presented in Table 6.4, and the no-load voltage from the segments is presented in Figure 6.5 and Figure 6.6.

Table 6.4 Data from tests with segments 1 and 2

Case	ψ_{rms}, [mVs/Hz]	E_{rms}, [mV/Hz]	Freq, [Hz]	I_{field}, [A]	U_{field}, [V]
Segment 1	0.088	0.088	166.7	4.0	7.5
Segment 1	0.159	0.159	166.7	8.0	15
Segment 2	0.06	0.06	166.7	4.0	7.5
Segment 2	0.107	0.107	166.7	8.0	15.0

The total flux linkage in stator segment 1 matched the size of the flux linkage in the outer pickup coils in the dummy winding tests.

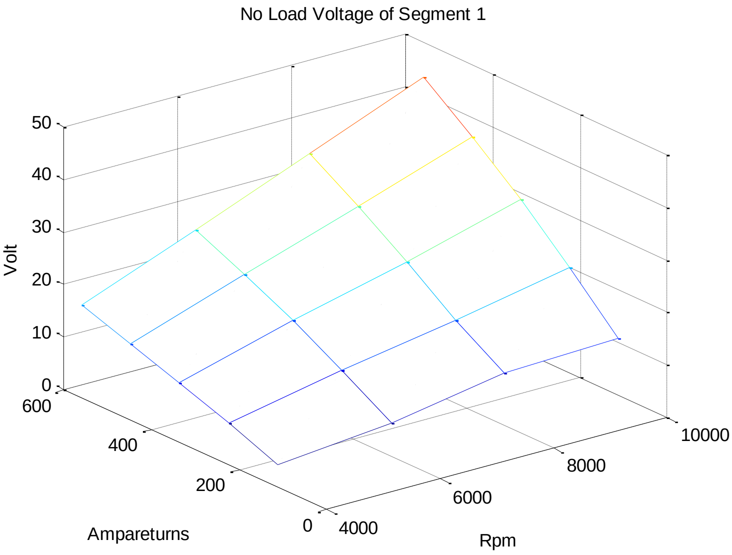

Figure 6.5 No-load voltage calculated from flux linkage measurements on stator segment 1 recalculated to fit the generator speed range.

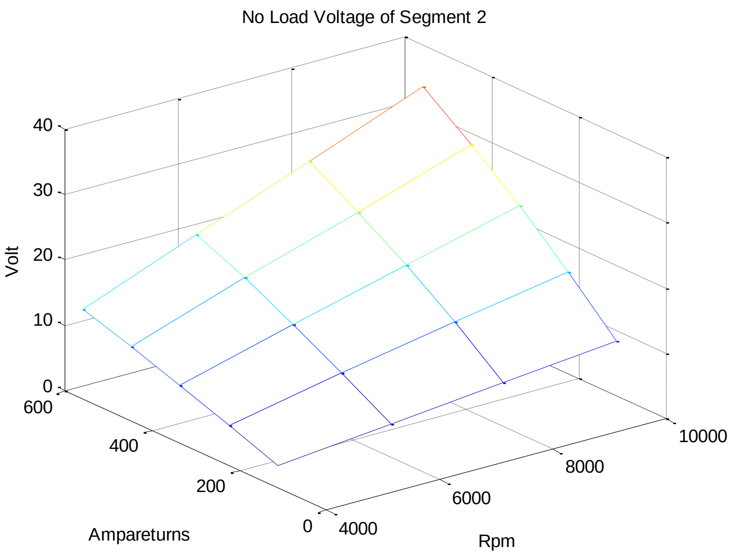

Figure 6.6 No-load voltage measurement calculated for stator segment 2.

As can be seen in Figures 6.5 and 6.6, neither of the segments would be capable of reaching 28.8 V at 4000 rpm without an increased magneto motive force, but Segment 1 with the handmade winding is closest to the target.

6.3 Power conversion tests

The factor of greatest interest when testing a generator is whether it can meet the power output specifications. During the electromagnetic tests of the stator, it became clear that the SM^2C-based generator would not be able to meet expectations regarding the induced flux linkage; however, it was still considered worth evaluating power output in stator segment 1, which had the most flux linkage.

The tests are performed with an excitation speed of 2000-4000 rpm and a rotor current of 2-10 [A]. The rotor has 56 turns in its winding, giving a magneto motive force of 112-560 [A_{turns}]. The no-load voltage and short-circuit current are measured, and the values used to calculate the maximum output power considering the resistive and reactive voltage drops in the stator. The results are presented in Figure 6.7**.**

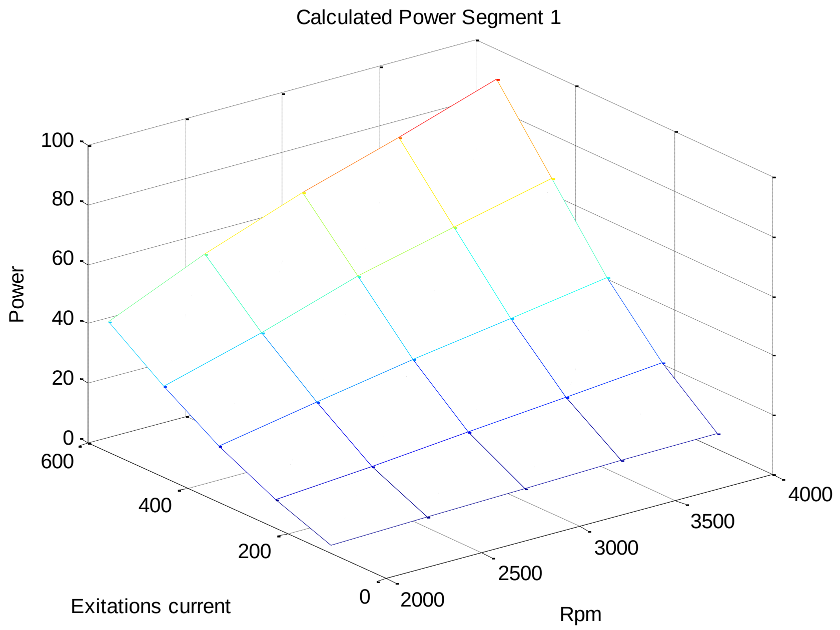

Figure 6.7 Calculated output power based on no-load voltage and short-cut current measurements on segment 1.

As shown in Figure 6.7, with calculated output power at 4000 rpm the generator segment would not be capable of producing the required output power required from the generator segment even if the excitation current is four times higher. The flux linkage in the stator segment is limited by the lack of ability of SM^2C to conduct magnetic flux, and the rotor saturation problem. As for now, there is no interest in evaluating the efficiency of the stator segment, as the excitation power is larger than the output power of the machine.

When these results are compared to the simulations in chapter 5, it is clear that the machine will not meet the requirements. The test results show that the induced voltage in a segment did not reach expectations.

6.4 Discussion and further analyses

It is clear that the intended generator design cannot fulfil the expectations of the design. To investigate why the design in Chapter 5 failed, new simulations investigating flux linkage are performed to allow a direct comparison with measured values from the moulded segment 1. It is of interest to see where in the design process the mistake was made. The simulations are performed with excitation currents giving a magneto motive force of 100-1500 [A_{turns}]. The main purpose of the simulations is to investigate the design of the generator and see if it is possible to verify the results from the EMF measurements of segment 1. This is achieved by comparing the flux linkage calculated from several new simulations. The simulations are performed with the three different SM^2C materials, one SMC P5 material from Höganäs, and laminated sheets M235-35A. Figure 6.8 presents a comparison of the results of these simulations with the flux linkage measured from segment 1 moulded with material SM^2C-G.

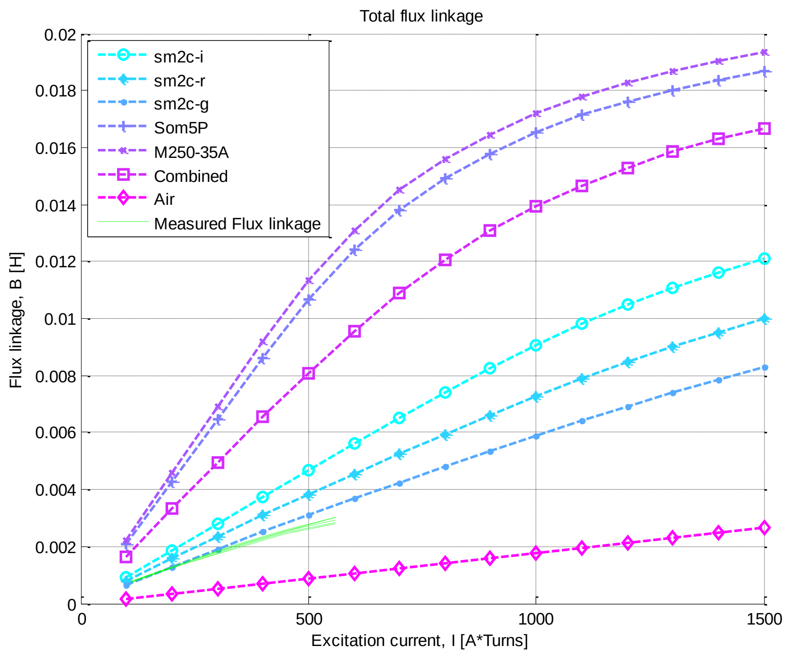

Figure 6.8 Simulated flux linkage with different core materials, compared with flux linkage measurements from segment 1. The “combined” material is a combination of different core materials where M250-35A is in the stator yoke, Som5P in the teeth, and SM^2C in the tooth tips.

The difference between the measured and simulated flux linkage results for the SM^2C-G material is due to an unexpected early saturation phenomenon at a low magnetisation current. The conclusion that can be drawn from this is that the simulation setup works, and the problems with power output in the generator design are not due to the selection of simulation program. There is a difference in material properties between the SM^2C-I and SM^2C-G materials, but this is not the major factor. It is likely that the problem lies in the selection of the mechanical design process of the generator.

6.5 Relative permeability and inductance

The intention of the generator design is to increase the usage of the 80 mm space available for the stator. A simulation comparing SM^2C material with several other core materials (Figure 6.8) showed that the highest flux linkage would be achieved by using M235-35A, also known as laminated sheets. The magnetic material in the core plays a significant role in the machine design. If the relative permeability is decreased, the output power will also decrease. This is more noticeable when generating power than when using power, as in motor applications.

The use of SM^2C material in the stator, with its low relative permeability, means that there is no possibility to take advantage of the low magnetisation current in the rotor to create a corresponding gain in EMF, as can be seen in Figure 6.9. The high rotor current density will lead to an increased rotor temperature as the magnetisation loss increases (see the thermal simulations in Chapter 5).

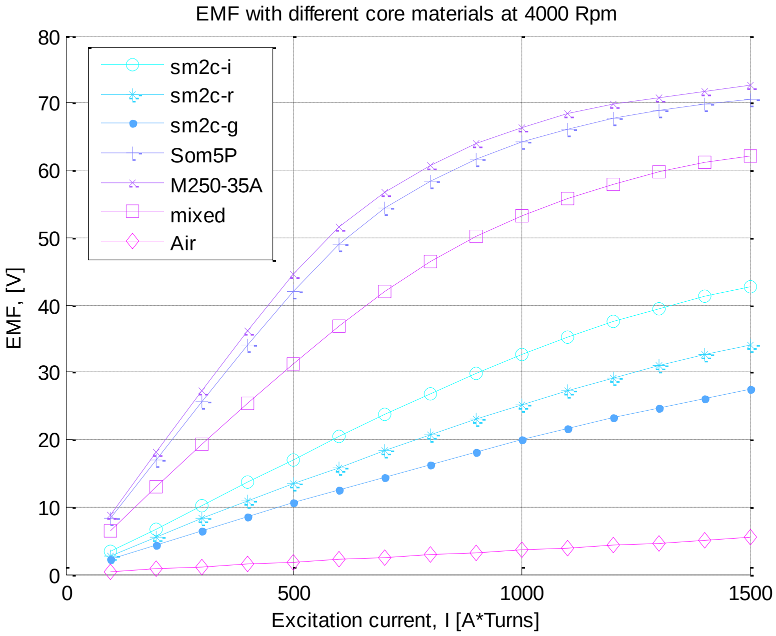

Figure 6.9 Simulated EMF_{rms} with different core materials. The combined material is in stator yoke: M250-35A, teeth: Som5P and tooth tip: SM^2C.

Assume that the core material changes from SM^2C to a high permeability material like M250-35A and the EMF increases roughly four times (see Figure 6.15) at an excitation current of 500 $A_{turns.}$ The question is whether using the magnetic properties of M250-35A in the stator core will meet the requirements of the intended generator.

A large relative permeability in the core material will increase the flux linkage and give a higher EMF in the winding. The excitation EMF in a generator is crucial for the possible amount of power conversion, especially if it is not connected to a grid from which it could use reactive power.

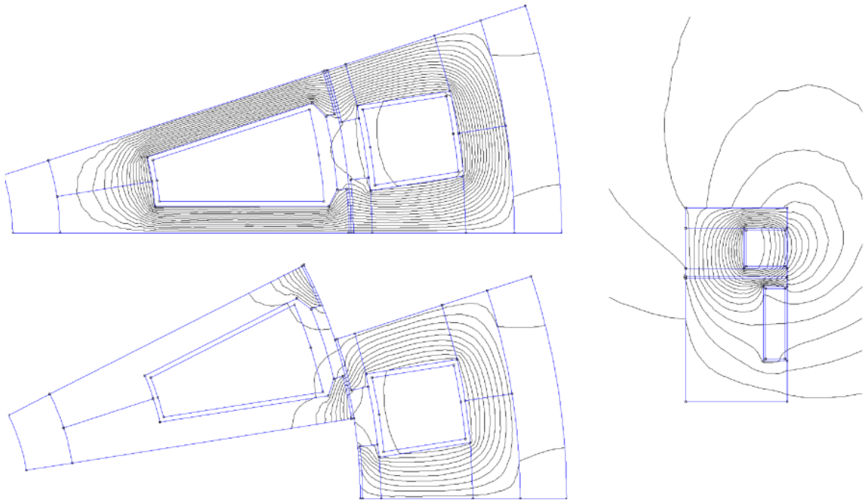

Figure 6.10 The three simulation models for calculating flux linkage and inductance.

With an increased permeability the inductance in the machine will change. The end turns in the generator design have a significant influence on the total inductance in a stator segment, especially in the segments moulded with SM^2C. To show this, a number of simulations are performed with three separate models: the first with stator and rotor aligned, the second with stator and rotor unaligned, and the third focusing on the end turns (see Figure 6.10). Figure 6.11 shows the inductance of the end turns and Figure 6.12 shows the total simulated inductance.

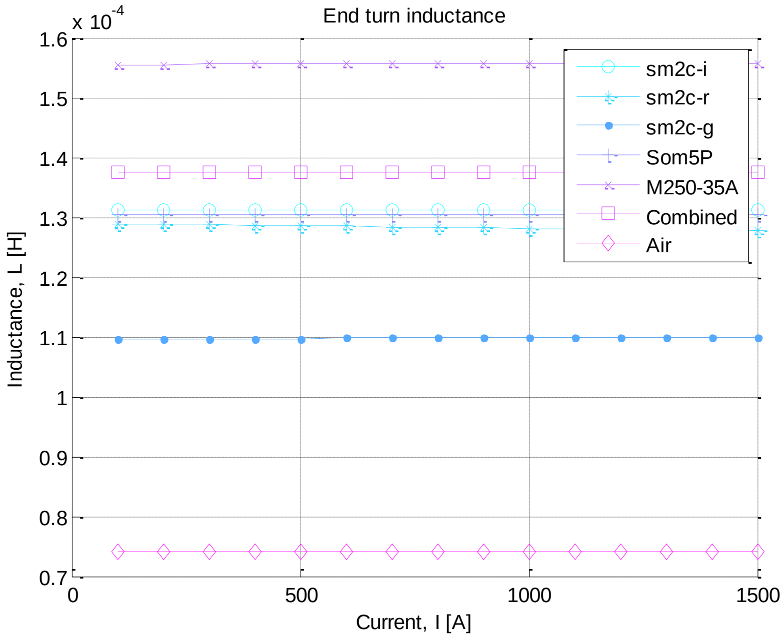

Figure 6.11 End turn inductance for different core materials.

As shown in Figure 6.11, the inductance in the end turns does not change significantly when different core materials are used. Hence, when using a core of high relative permeability, less of the voltage is used by the end turns.

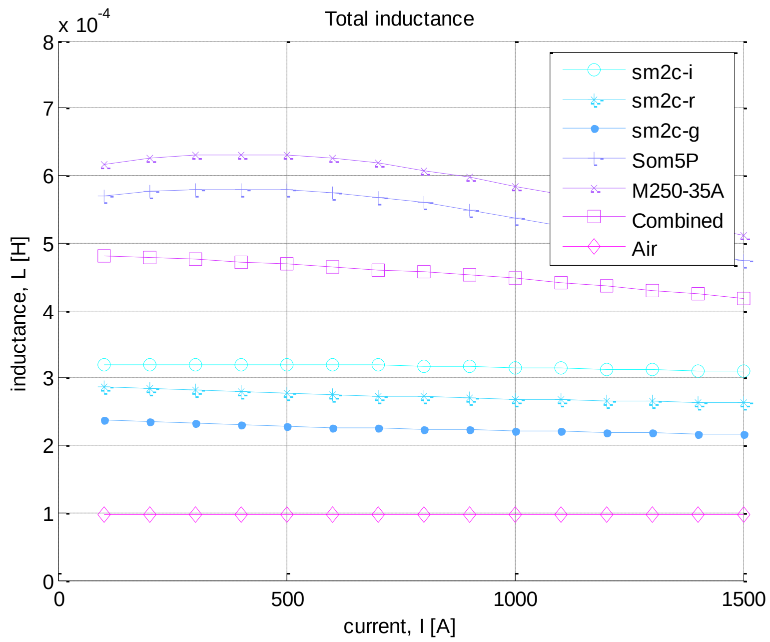

Figure 6.12 Total inductance in a segment with different core materials.

As shown, the end turn inductance is about half of the total inductance in the case of SM^2C materials. This would not be a problem if the contributed flux linkage in the end turns was large, but this is not the case (see Figure 6.13 compared to Figure 6.14). The end turns account for too large a proportion of the inductance without adding to the performance of the machine, and so this specific construction with three short axially placed segments in the generator is not compatible with SM^2C materials.

The question still remains of whether there is a possibility to save the generator construction by increasing the relative permeability in the core material in order to increase the flux linkage.

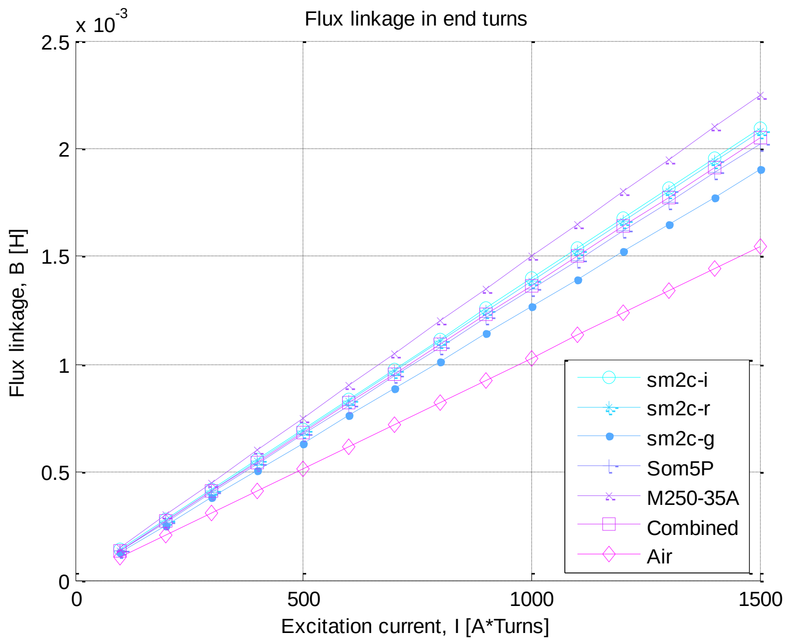

Figure 6.13 Flux linkage in the end turns for a segment with a winding of 15.5 turns, for core materials.

As shown in Figure 6.13, the flux linkage in the end turns does not change significantly with different core materials. This means that the inductance in the end turns does not play a significant role in total inductance as relative permeability increases.

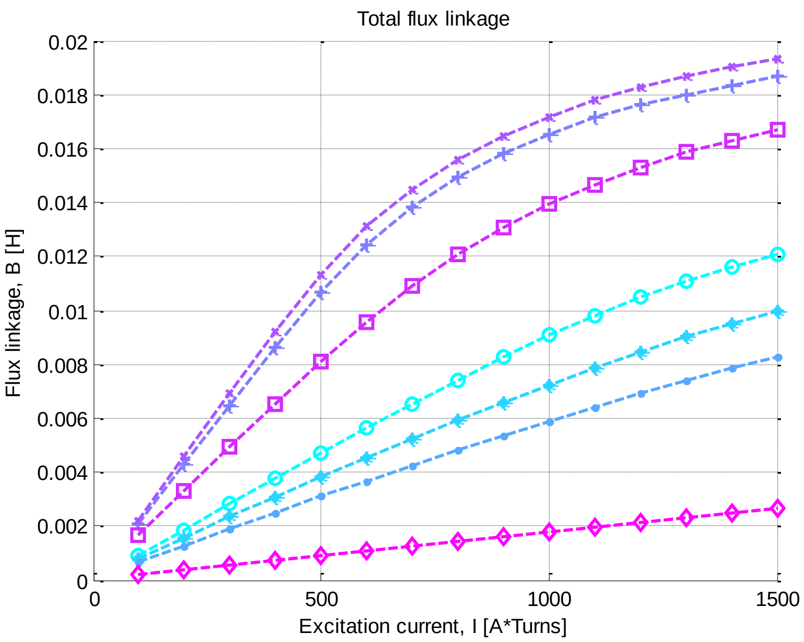

Figure 6.14 Total flux linkage in a segment with 15.5 turns in the winding, for different core materials.

The impact of different core materials in the generator design is investigated using the circuit design simulator LT-Spice. Two models were constructed: one for the phase equivalent circuit of the synchronous generator (see Figure 6.15) and the other for the full generator model (see Figure 6.16).

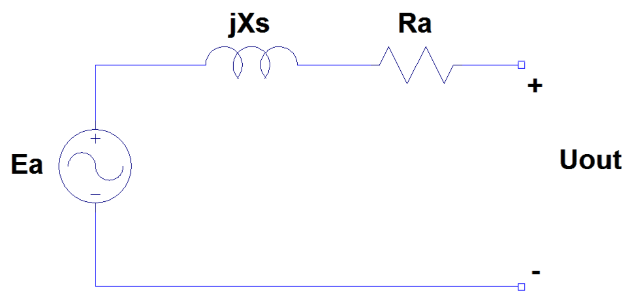

Figure 6.15 The equivalent phase circuit for the synchronous generator.

With current direction references, the equivalent circuit equation of the model becomes:

$$\vec{U}_{out} = \vec{E}_a - (R_a + jX_s) \cdot \vec{I}_a \qquad (2)$$

In a synchronous generator, the winding reactance is usually much larger than the resistance in the winding, and so this equation can be rewritten as:

$$\vec{U}_{out} = \vec{E}_a - jX_s \cdot \vec{I}_a \qquad (3)$$

The phase equivalent circuit is used to verify the full generator model, as it is easy to compare with the measured no-load voltage used to calculate the power in Figure 6.7. The comparison is presented in Table 6.5.

Table 6.5 Verification of the phase model with an external load resistor.

EMF, rms [V]	Freq [Hz]	Inductance [mH]	Measured output power [W]	Simulated output power [W]
6.36	333	0.191	44	44.4
7.88	416	0.184	57.5	57.7

9.26	500	0.179	69.3	69.3
10.4	583	0.171	79.2	79.1
11.7	666	0.168	90.3	90.0

Verifying the phase model and making comparison with several measured values allows use of the full generator model for further investigation of whether the required output power might be achieved by using a different core material with higher relative permeability in the segments.

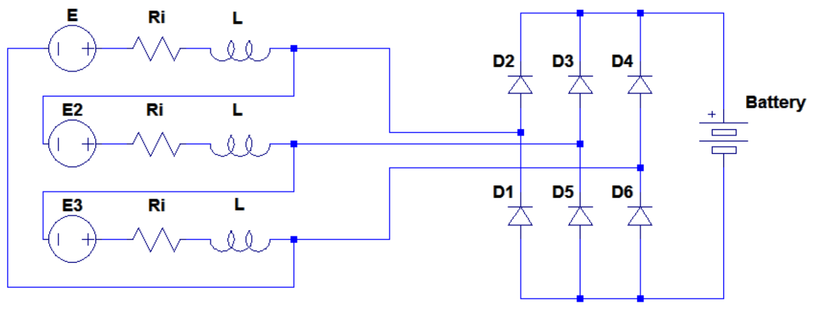

Figure 6.16 Model of the automobile generator with rectifier bridge and battery.

The two LT-Spice models make it possible to calculate the output power with the rectifier bridge and the maximum output power with a resistor as a load without the battery and the rectifier bridge.

Table 6.6 Simulated output power with different core materials at a nominal speed of 666 Hz and a maximum three-phase output power without the battery and rectifier bridge as comparison.

Core material	EMF , rms [V]	Inductance [mH]	Output power with rectifier bridge [W]	Maximum output power [W]
SM^2C-G	27.5	0.217	830	1170
SM^2C-R	35	0.263	1350	1584
SM^2C-I	43	0.310	1650	2361
Som5P	70.5	0.475	2080	3645
Combined	63	0.418	2100	3270
M250.35A	73	0.512	2010	3618

The difference in output power when the rectifier and battery are used is related to the clamping of the terminal voltage that the battery applies and the number of turns in the winding. Since the impedance in the generator is basically inductive, the voltage level corresponding to the maximum output power is the EMF divided by the square root of 2, as seen in Figure 6.17. The battery has a significantly lower voltage than the voltage level at maximum output power. This gives a current level close to the short-circuit current, which cannot fulfil the requirement for the generator.

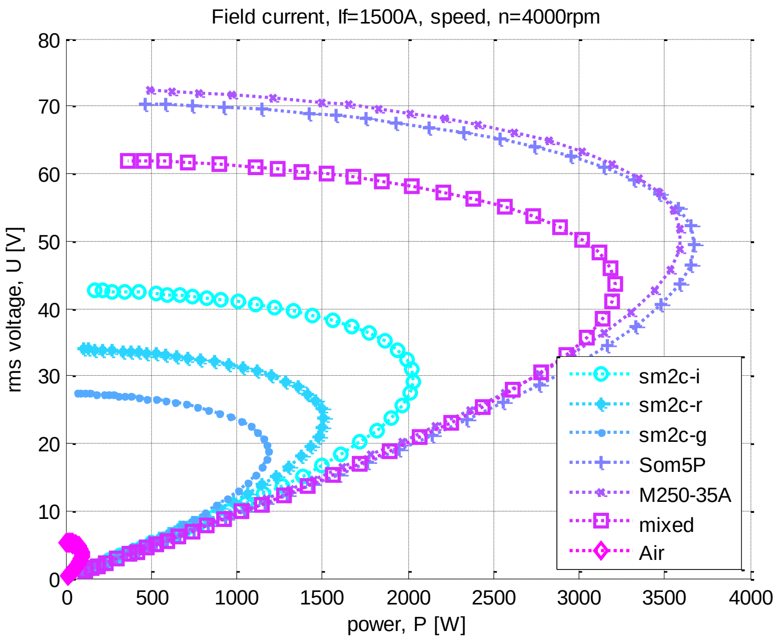

Figure 6.17 Power versus voltage curve for the different core materials at maximum excitation current.

The answer to the question of whether changing the material in the core will meet the requirements of the generator is thus **yes!** By adjusting the number of turns in the winding to fit an output voltage of 28 V (see Figure 6.18), it is possible to meet the output requirement of 3000 W using M250-35A and Som5P (see Table 6.7).

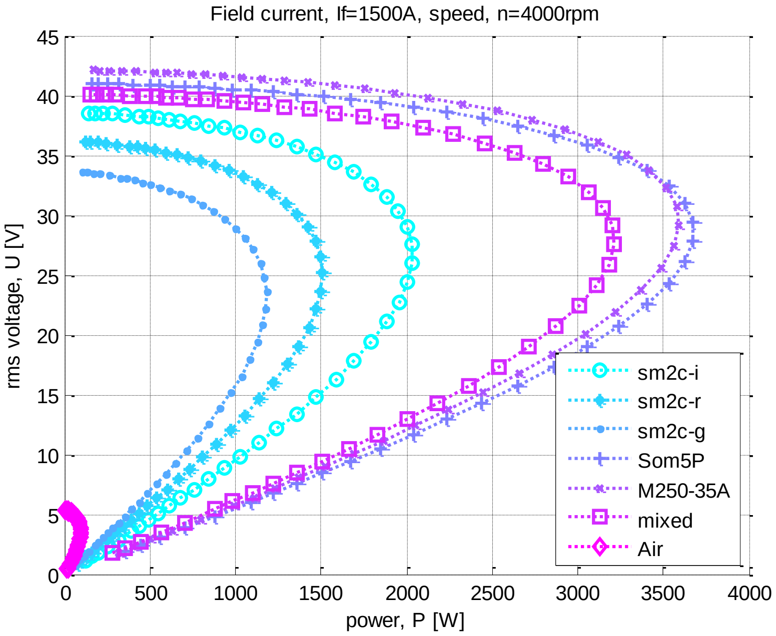

Figure 6.18 Adjusted PV curve for the different core materials at maximum excitation current.

Table 6.7 Simulated output power with different core materials with conditioned number of turns in the winding for 28 V at nominal speed 666 Hz and maximum three-phase output power without the battery and rectifier bridge as comparison.

Core material	EMF , rms [V]	Inductance [mH]	Output power With rectifier bridge [W]	Maximum Output power [W]
SM^2C-G	31.9	0.252	988	1170
SM^2C-R	35	0.263	1350	1584
SM^2C-I	38.8	0.253	1659	2361
Som5P	40.9	0.16	2951	3645
Combined	40.6	0.174	2744	3270
M250.35A	42.4	0.173	2979	3618

It is possible that the decreased number of turns in the winding will create problems in the manufacturing of the winding, but at least it is theoretically possible.

The original SM^2C design described in Chapter 5 did not meet the requirement because the simulations focused on the maximum torque at nominal speed, in order to calculate the nominal output power. This method of designing the machine is not suitable, since the armature reaction is not accounted for. When this is corrected, the result is also in accordance with the experiments and the need for high excitation levels is correctly accounted for.

6.6 Summary

It is clear from the tests described in this chapter that the generator designed with SM^2C as core material does not fulfil the requirements. The design process is at fault here, as the low flux linkage in combination with the large end turn inductance cannot sustain the amount of required output current. Furthermore, the SM^2C material is not compatible with the prototype generator construction due to its low relative permeability. However, the axially-stacked stator segment design still has several interesting aspects, especially with a different selection of core material in the stator, making it possible to achieve the intended output power. One of these interesting aspects is manufacturability, which is especially interesting to investigate further with a laminated winding.

Chapter 7

Laminated Windings

This chapter describes a winding that has outstanding geometric accuracy and good conductor fill factor, and that is very suitable for production. These are all characteristics that are needed in a winding for a machine made of soft magnetic composite. However, this winding is not limited to SMC applications alone; the magnetic core of the machine can be made from a combination of different materials such as lamination sheets, SMC, SM^2C, and air.

7.1 Winding design

Laminated windings are based on an ordinary copper foil. Sections are punched in the foil to shape the winding, and then the foil is rolled up to form a finished winding with outstanding accuracy in geometric shape and form compared to ordinary windings (see Figure 7.1). This geometric accuracy makes the laminated winding highly suitable for use in electrical machines with core materials such as SMC and SM^2C.

When designing a laminated winding, the distance between each punched section will grow with each winding layer. To adjust for this and align the winding turns to fit together with the magnetic core, the distance between the punches needs to increase with every turn. With this winding design method, there is a possibility to predetermine the slot fill factor in the machine, depending on the intended application of the machine. With a high slot fill factor, the winding will be suitable for SMC and SM^2C machines.

Figure 7.1 A laminated winding made from a rolled-up punched/cut strip.

This production method allows for space to be incorporated between each winding turn to create a rapid cooling capability, by means of air blown in between the winding turns. There is also the possibility to choose where in the windings the cooling will be applied. This can be accomplished by controlling the distance between the layers to create one or several larger openings in the winding, which need not necessarily be equally distributed. The cooling medium can thus be applied specifically where the heat develops. However, all this comes at the expense of the slot fill factor in the winding. See Figure 7.2.

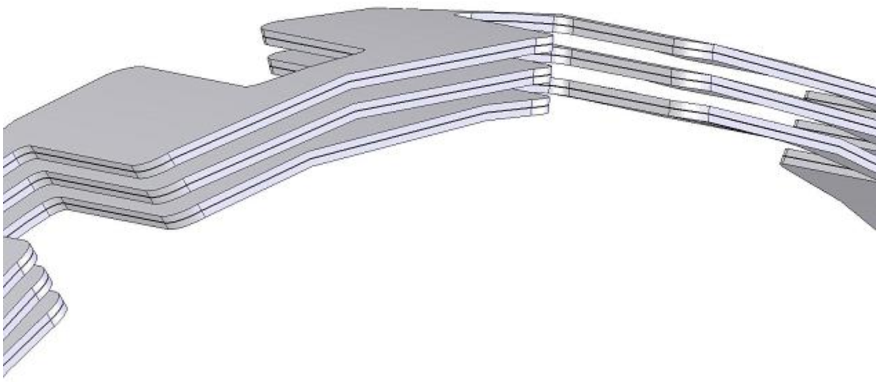

Figure 7.2 Openings in the laminated winding to create channels for the cooling air flow.

The incorporation of an effective cooling method directly into the laminated winding means that the active length of the machine can be increased by minimizing the winding end turns, which would not be possible with an ordinary winding made of continuous round conductors. This is achieved by varying the cross-sectional area of the conductor; one size is chosen in the area where the cooling is applied and another cross section area size in the end turns of the winding (see Figure 7.3). The thermal stress in the end turns is increased, but this problem is limited by the fast transport of heat to the cooling area.

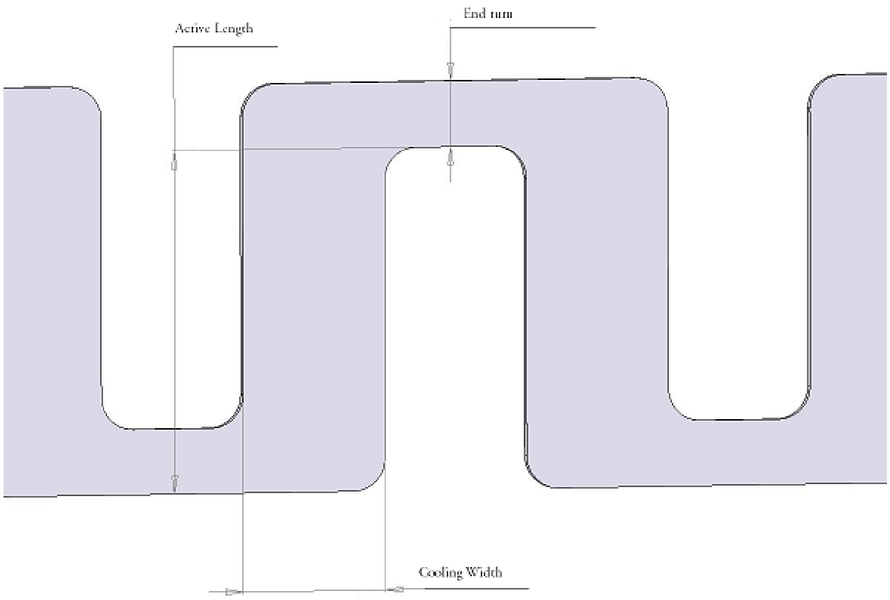

Figure 7.3 Increasing the active length in a punched-foil laminated winding.

7.2 Winding materials

The production process of the laminated winding, along with the possibilities it offers for effective cooling of the machine, suggests that aluminium could be an interesting material to use. There are several advantages of using aluminium as winding material instead of copper:

- The market price difference between copper and aluminium, together with the difference in density and resistance between the two materials, means that at the time of writing copper is about 7 times as expensive as aluminium.

- A good insulation can be achieved by enhancing the natural oxidization layer on the aluminium conductor [6]. Using this oxidation layer as insulation has the advantage of an increased thermal conductivity in the insulation, compared to other common types of coating.

- Aluminium has 64% more resistivity than copper, which provides a natural defence against eddy current losses with increased electric frequency [5].

- The density of aluminium compared to copper contributes to lightweight windings and thereby less weight in the finished machine.

All of these advantages make aluminium highly appealing as a winding material. However, it also has some drawbacks, the most significant being its 64% increase in DC resistance compared to copper. This indicates that when aluminium is used in windings without an increased cooling capability, in order to avoid increasing the power loss in the winding the slot fill factor needs to be increased by 64%.

7.3 Prototype production

A prototype laminated winding is created for the generator design described in Chapter 5. The geometry of the winding is given in Table 7.1.

Table 7.1 Prototype laminated winding

Property	Value	[unit]
Thickness of winding material	0.5	[mm]
Thickness of winding	8	[mm]
Number of turns	12	
Thickness of electric isolation material	0.03	[mm]
Thickness of air layer between turns	0.05-0.15	[mm]

The prototype windings are made with a two-stage punching/cutting method. In the first stage, the space allocated for the magnetic core in the electrical machine is punched on one side of the strip with the distance of a pole-pair between the punches. Compensation was made for the fact that this distance increases with each winding turn, depending on the size of the winding and thickness of the strip. In the second stage, the winding is completed by punching the second side to the strip and placing the winding slots between the first punches on the opposite side (see Figure

7.4). After finishing the strip, any burrs were removed. Two of the prototype windings are electrically insulated turn to turn with a thin tape and tested regarding the possibility of rapid cooling.

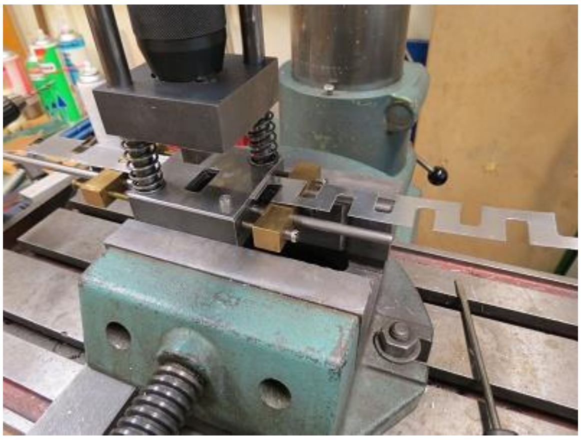

Figure 7.4 Cutting the second side to finish the strip before using it to form a winding.

7.4 Cooling tests

A number of transient thermal measurements were performed on two laminated windings: one made of aluminium and one of copper. The test bench for the thermal measurements is made up of one variable transformer connected to a 230 V_{AC} grid on the primary side. On the secondary side, two transformers connected in series to deliver a 70A/50Hz current at very low voltage are connected to the winding. An infrared camera is used to measure thermal events, together with two multimeters to give an overview of the power applied to the winding and to compare the thermal measurement from the infrared camera with a thermo element. Two ampere meters are used to measure the current on the primary side and on the secondary side. See Figure 7.5.

Figure 7.5 Setup for the thermal tests.

During the tests, the current densities in the conductors were 10–14.4 A/mm^2 and the air flow through the winding has a velocity of 0-1.5 m/s. The heating processes are observed using a temperature sensor and an infrared camera (see Figure 7.6).

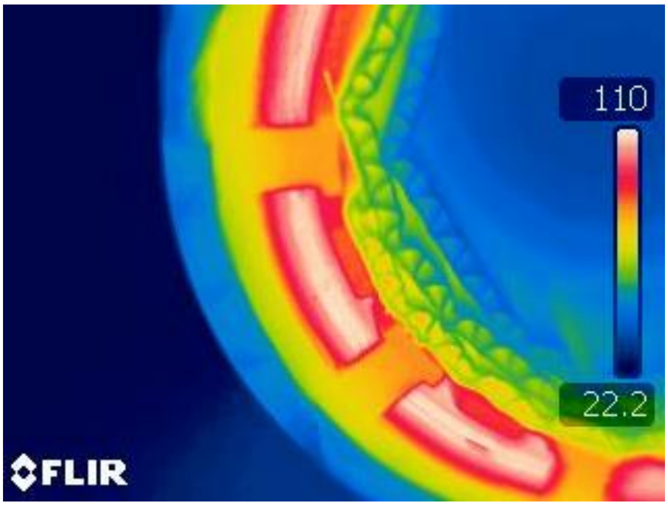

Figure 7.6 An infrared picture of the thermal development in the machine without cooling.

The infrared camera greatly facilitated the measurement, allowing visualization of the thermal processes in the assembled winding to help understand the thermal development of the machine. A MATLAB script was used to analyse the film and plot the thermal development from the tests. The thermal measurement results are presented in Figure 7.7.

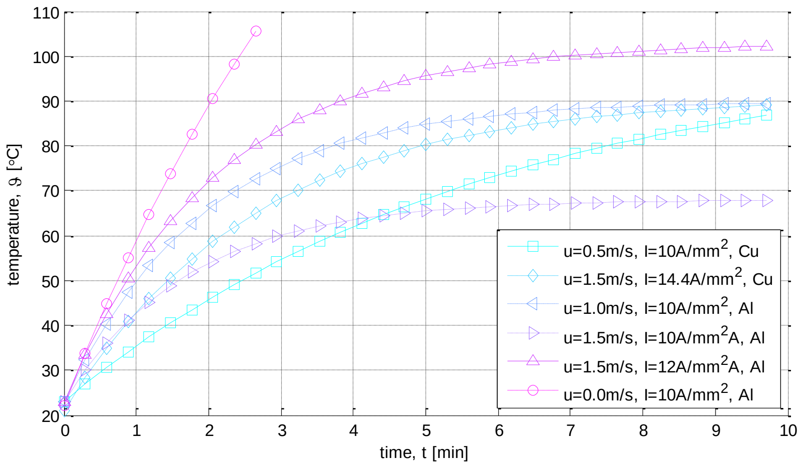

Figure 7.7 Thermal test results with current densities of 10-14.4 A/mm^2 and air flow velocities of 0-1.5 m/s.

The average air speed is measured just after it leaves the winding. Due to the winding geometry, the air speed between the turns can be calculated as:

$$V_{Lair} = V_{out} \frac{A_{Th} \cdot W_{TH} \cdot I_{Th}}{A_{Th}}$$

Where:

V_{Lair} = Air speed between the layers in the winding

V_{out} = Air speed outside the winding

A_{Th} = Air layer thickness between the winding turns

W_{Th} = Winding turn thickness

I_{Th} = Insulation thickness

7.5 Summary

This chapter shows that laminated windings offer the possibility of increasing the accuracy of the geometric winding tolerances, which in turn will improve the performance of electrical machines moulded from SMC and SM^2C. With the production method described here, the laminated winding also has the ability to give a high coil fill factor.

It appears to be possible to remove the heat that develops directly in the winding slot by passing air through the winding. While aluminium windings develop more heat than copper windings, due to the increased resistance of aluminium compared to copper, the aluminium winding still has a significant possibility for enhanced cooling. The weakness of the punching/cutting production method is the possibility of burrs, which will weaken the dielectric strength in the insulation layer if anodizing is used as insulation. Aluminium is a very interesting material for creating laminated windings, due to the simplicity of making the winding combined with the price difference between the two materials. Some aspects of laminated windings still remain to be investigated, such as the cooling properties of the winding as a function of the length of the winding, since length increases the air flow resistance.

Chapter 8

Conclusions

This thesis presents the challenges and benefits in designing electrical machines using a moulding technique with SM^2C. The thesis also describes the moulding technique, winding layouts, and practical suggestions for increasing the possibility of small-scale production. The development in winding technology led to the design of the laminated winding, which has a great potential in direct efficient cooling.

8.1 Summary of results

The main conclusion is that at the time of writing, the relative permeability of the SM^2C material is too low for it to make a serious contribution to electrical machine designs, even though it has several interesting features. However, the laminated winding shows promising results in terms of production suitability, heat dissipation by cooling directly in the winding slot, and the possibility to utilize aluminium as winding material. Aluminium has a number of advantages, including the option of using aluminium oxide as a dielectric protection and thereby increasing the thermal conductivity in the winding.

Moulding

During the experimental moulding work it became clear that it is not a simple task to control the end result of moulding a magnetic core for electrical machines. The relative permeability in the material can change from one moulding to the next due to the iron powder placement in the mould, which affects the density of the SM^2C material. The geometric form of the mould is highly unconstrained, and the moulding process would be easily controllable if the task were only to mould separate building blocks from which to build a stator. The introduction of inserts into the mould increases the complexity of the moulding and makes it more difficult to achieve consistent results.

Windings

The winding in moulded machines are constructed before the core, and play a crucial role in controlling the machine topology to achieve repeatable results in terms of the performance of a moulded machine. The winding thus needs to have a stable geometry with good geometric tolerances. The winding design should be selected with care, and the mechanical machine design should always start with the winding; the machine should be built from the perspective of the winding. When selecting the winding layout for moulding, it is important to keep in mind the manufacturability of the winding or the winding segments.

Laminated winding

Laminated windings fulfil many of the aspects needed in windings for moulding electrical machines, but they also offer the possibility of direct, efficient cooling directly in the winding slot, which will be lost if the winding is incorporated into a moulded machine. The geometric accuracy of the winding is outstanding, which will give a high conductor fill factor. The geometric accuracy of the winding should also make it possible to make a high-efficiency compact machine, but this remains to be investigated further. The use of aluminium to construct the winding makes it possible to reduce the material cost and thereby to decrease the production cost of the machine. The laminated winding has a very stable form. Ways to build the magnetic core around the winding also need to be investigated further.

8.2 Future work

If SM^2C materials are to be used in moulded rotated electrical machines, some way must be found to increase their relative permeability. It would be interesting to see whether using the SM^2C material in air winded machines would give an advantage to their kind of machine topology.

There are several interesting aspects of laminated windings that remain to be investigated, not least their cooling capabilities and the possibilities they offer for the mechanical design of the iron core. In terms of cooling the winding, the possibility should be explored of cooling with different media such as air, oil, and so on. There is also a need to investigate how the length of the machine affects the air cooling in the machine.

Another aspect of cooling that would be of interest to explore is the issue of how the cooling is applied in the winding. The cooling openings in the winding can be one larger opening or several smaller openings. It would also be useful to see whether the cooling needs to be applied over the whole winding, or if it will be enough to cool only in several selected areas. The choice of material from which to construct the winding is also a highly interesting aspect for further investigation; particularly aluminium, and the advantages it can give both in money savings and in the possibility to use aluminium oxide as dielectric insulation.

It would be interesting to investigate more mechanical designs of a laminated winding, where the winding layout is based on modular and circumferentially distributed coils.

The mechanical design of an iron core that is compatible with the laminated winding is a particularly important challenge, especially in combination with the requirement for manufacturability. The possibility to use combinations of different core materials in the core design can be an advantage in machine design.

References

[1] TORD CEDELL, PETER JEPPSSON, MATS ANDERSSON, JAN-ERIC STÅHL MATS ALAKÜLA, AVO REINAP, CONNY HÖGMARK (2009), "NEW ADVANCES IN SOFT MAGNETIC ATERIALS – PROPERTIES OF MOULDED FLUX CONDUCTERS IN INDUKTORS AND ELECTRICAL MOTORS" INDUCTICA TECHNICAL CNFERENCE, (2009) BERLIN GERMANY

[2] PETER JEPPSSON, TORD CEDELL, MATS ANDERSSON, MATS ALAKÜLA, AVO REINAP (2007), " INJEKTION MOULDING OF MAGNETIC FLUX CONDUKTERS BASED ON SOFT MAGNETIC COMPOSITES" SPS 2007 GÖTEBORG

[3] PETER JEPPSSON, MATS ANDERSSON, TORD CEDELL, MATS ALAKÜLA, AVO REINAP (2009), " ROTOCAST – A NEW METHOD TO PRODUCE OPTIMALLY PACKED SMC COMPONENTS 2009 GÖTEBORG

[4] LEIF SVENSSON, MATS ANDERSSON, TORD CEDELL PETER JEPPSSON, , ANDERS FRÖJVIK (2011), " ELECTRICAL ISOLATION OF COILS IN SMC APPLICATIONS" 2011 LUND

[5] CHARLES R. SULIVAN "ALUMINUM WINDINGS AND OTHER STRATEGIES FOR HIGH-FREQUENCY MAGNETICS DESIGN IN AN ERA OF HIGH COPPER AND ENERGY COST" IEEE TRANSACTIONS ON POWER ELECTRONICS 2008

[6] H. F. CHURCH "THE DIELECTRIC PROPORTIES OF ANODIC ALUMINIUM OXIDE FILMS" – THE INSTITUTION OF ELECTRICAL ENGINEERS 1961

[7] AYMAN M. EL-REFAIE "FRACTIONAL-SLOT CONMOTORS AND CHALLENGES" – IEEE TRANSACTIONS ON INDUSTRIAL ELECTRONICS, VOL. 57 NO. 1 JANUARY 2010

[8] AVO REINAP, DAN HAGSTTEDT, CONNY HÖGMARK, MATS ALAKÜLA "SUB-OPTIMIZATION OF A CLAW-POLE STRUCTURE ACCORDING TO MATERIAL PROPERTIES OF SOFT MAGNETIC MATERIALS" – IEEE TRANSACTIONS ON MAGNETICS, VOL. 48 NO. 4 APRIL 2012

[9] AVO REINAP, DAN HAGSTTEDT, CONNY HÖGMARK, MATS ALAKÜLA "EVALUATION OF A SEMI CLAW-POLE MACHINE WITH SM^2C CORE" – NIAGARA FALLS, ONTARIO, CANNADA, MAY 15-18 2011

[10] JE'RÖME CROS, PHILIPE VIAROUE "SYNTHESIS OF HIGH PERFORMANCE PM MOTORS WITH CONCENTRATED WINDINGS" – IEEE TRANSACTIONS ON ENERGY CONVERSION VOL. 17 NO. 2 JUNE 2002

[11] REINAP A., ALAKÜLA, M., LINDSTEDT, G., THURESSON, B., CEDELL, T., ANDERSSON, M., JEPPSSON, P. "AN INTEGRATED DESIGN OF A MACHINE WITH SOFT MAGNETIC MOULDABLE COMPOSITE". INTERNATIONAL CONFERENCE ON ELECTRICAL MACHINES (ICEM2008), VILAMOURA, PORTUGAL, SEPT. 6-9, 2008.

[12] REINAP, A., HÖGMARK, C., ALAKÜLA, M., CEDELL, T., ANDERSSON, M., JEPPSSON, P. (2008), "DESIGN AND PROTOTYPING A TORUS MACHINE WITH A ROTOCAST CORE". INTERNATIONAL CONFERENCE ON ELECTRICAL MACHINES (ICEM2008), VILAMOURA, PORTUGAL, SEPT. 6-9, 2008

[13] POMPERMAIER, C., SJÖBERG, L., NORD, G., "DESIGN AND OPTIMIZATION OF A PERMANENT MAGNET TRANSVESE FLUX MACHINE". INTERNATIONAL CONFERENCE ON ELECTRICAL MACHINES (ICEM2012), MARSEILLE, FRANCE, SEPT. 2-5, 2012.

[14] MÜLLER, C., KALKMAN, B., SONTHEIM, J., "A HIGHLY INNOVATED TRANSVERSAL FLUX MOTOR DESIGN WITH INTEGRATED INVERTER". INTERNATIONAL ELECTRIC DRIVES PRODUCTION CONFERENCE (EDPC2012), NUREMBERG, GERMANY, OKT. 15-18, 2012.

Appendix A

Analysis and tests of a transversal flux machine (TFM) with wave-winding

The test object is analysed in two ways: on the one hand as a stator segment with soft magnetic mouldable core and on the other as an electrically magnetized synchronous machine. Either way, the practical experiments on a single-phase motor segment are useful in evaluating the assembly process of the designed machine: a three-phase electrically magnetized synchronous machine made of a number of modular semi-claw pole stator segments.

Some reflections on the tests, and future possibilities:

- Improve the magnetic coupling in order to get more out of the machine; consider inserts in the stator.
- Analyse the rotor core geometry and material properties in order to extend the linear relationship between the excitation field and current.
- Once again, consider the manufacturability of the high-fill high-tolerance winding that reduces the DC power loss in the windings.

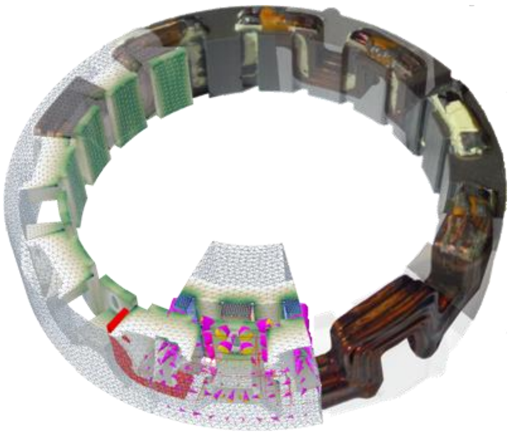

Chronology and outcome of experimental verification

Starting from the formation of a winding and a stator core, the introductory work is followed up with an evaluation of the core by using a provisional permanent-magnet excited surface-mounted magnet ring. After construction of the first provisional electrically magnetized rotor the permanent-magnet rotor is excluded from the experiments. The next main steps of the experimental development are as follows:

1. Formation of wave winding by using different conductor profiles

    a. Pro: Successful deform and wind up concept, acceptable fill factor.

    b. Contra: A non-industrial process which takes advantage of 3D-printed dummy windings.

2. Learning the quality of moulding processes for a complex core (ST1, ST2, later ST4)

    a. Pro: Perfect formation of core parts such as tooth-tips.

    b. Contra: Magnetic permeability approximately 30% lower than in test tubes, huge leakage, considerable difference between the batches.

3. Moulding and testing the actual winding (ST3)

electromechanically and thermal.

a. Pro: Improved knowledge of material properties by involving the thermal experiments and verifying the EMF measurements.

b. Contra: Discrepancy between theoretically expected (test geometry) and practically verified (application geometry) material properties.

4. Focus on spectral characteristics of moulded windings

   a. Pro: The winding works as an inductive load on a wide scope of low frequencies (below 1Mhz).

   b. Contra: Incomplete knowledge on frequency response for higher frequencies.

5. Investigation of electrically-magnetised rotor including the development of stator windings and segments (ST5)

   a. Pro: Modular construction for the rotor core.

   b. Contra: prototyping of rotor windings with an intended high fill factor; the first two tests ended with fill factors of 7% and 21%, respectively. The rotor core becomes saturated faster than expected at 500 Aturns. The rotor core has unknown material properties, which should be investigated.

6. Focus on increasing the magnetic coupling by improving the magnetic permeability of the core parts

   a. Pro: Parallel production of the magnetic core and winding by introducing modular stator halves.

   b. Contra: The implementation of two stator halves may result in lower performance due to the axial air-gap between the core halves.

Prediction of generator characteristics at 4krpm

As the final goal of the design is an electrically magnetized synchronous machine (EMSM) in generator operation, the corresponding loading characteristics are predicted at the nominal speed of 4krpm. A TFM with wave-winding, a resistance of 0.052Ω and an inductance of 163.9μH, is analysed as a 20-pole generator winding at 4krpm. The flux linkage is modelled at two different levels (10 and 5 mVs), which are shown as solid and line thickness respectively in the figure below.

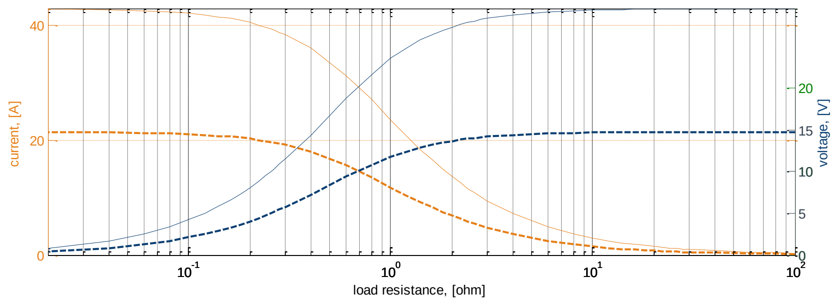

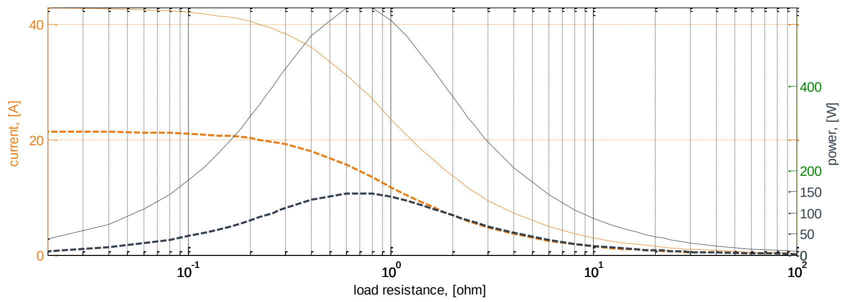

By doubling the flux linkage, the output power of the winding will be achieved.

Imax=[42.9 & 21.5] A, Umax=[29.6 & 14.8] V, Pmax=[586.3 & 145.5] VA

Other test goals to be analysed are lacking experimental flux linkage data.

N=16, R=0.037 Ohm (0.034 Ohm), L=58uH, 57.7 uH, C=8.14 mF, 0,4 mF

N=18, R=0.049 Ohm, L=72mH, 73mH

First generator test with permanent-magnet rotor

A prototype rotor is constructed with 12 of the total 20 magnets to magnetize a permanent-magnet rotor. The permanent magnets are shifted so that the first and the last of the 12 magnets have the outer edge in the angular direction aligned with the outer edge of the tooth-tip. This causes the back EMF to be more sinusoidal and also slightly smaller, compared to a magnet arrangement where the middle line of each magnet is perfectly aligned with the middle lines of the tooth-tips see figure below.

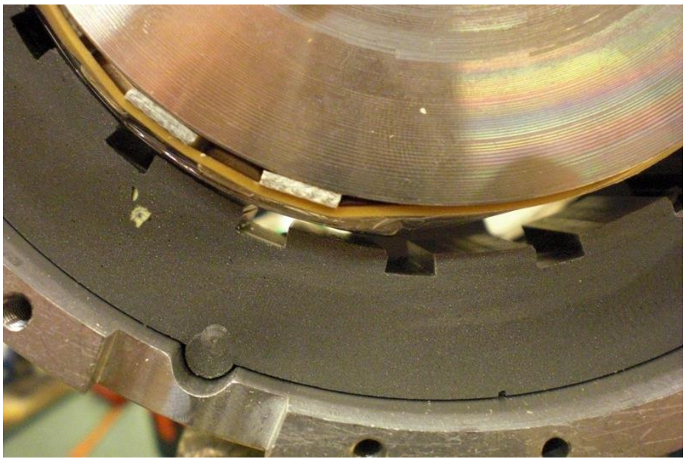

Back EMF measurement for the stator module with 15.5 turns (ST3)

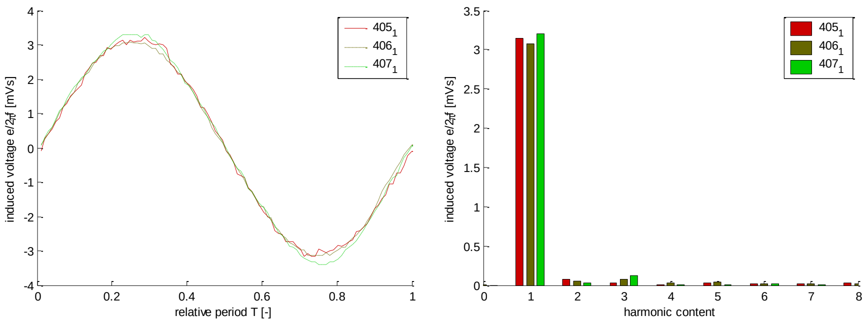

Test	ψ_{m1}	ψ_{rms}	ψ_{thd}	U_{m1}	U_{rms}	U_{thd}	If	Uf	F

	mVs	mVs	%	mVs	mVs	%	A	V	Hz
05	3.15	2.21	0.0	3.15	2.20	0.1	0	0	29.9
06	3.11	2.18	0.0	3.11	2.18	0.1	0	0	74.9
07	3.30	2.31	0.0	3.27	2.29	0.1	0	0	75.1

110302

Considering the presence of all magnets, the corresponding maximum flux linkage is 5.35 mVs. By increasing the amount of permanent-magnet material so that there is no lateral air-space between the magnets, the maximum flux linkage can be increased to 8.92 mVs.

First generator test with electromagnetic rotor

The slot area of the rotor core intended for the winding is estimated to be 128 mm^2. The rotor winding is made of 18 turns and thereby establishes an conductor area on 9 mm^2 of pure copper with a 7% fill factor (see figure below). The highest excitation current used in the tests, which is above 8.5 A, gives a current density of 17 A/mm^2 and more than 153 A of magneto motive force.

Back EMF measurements at different excitation currents for the stator module with 15.5 turns (ST3).

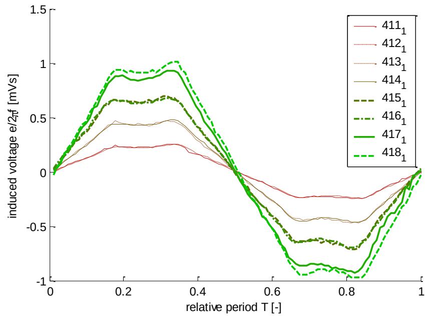

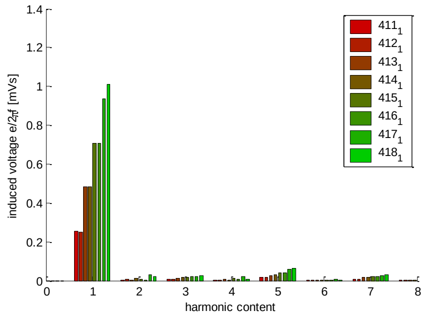

Induced voltage per excitation speed (fft, thd, rms)

Test	ψ_{m1}	ψ_{rms}	ψ_{thd}	U_{m1}	U_{rms}	U_{thd}	If	Uf	F
	mVs	mVs	%	mVs	mVs	%	A	V	Hz
11	0.26	0.18	0.0	0.25	0.18	0.6	2.24	1	75.4
12	0.25	0.18	0.0	0.25	0.18	0.7	2.24	1	243.3
13	0.49	0.34	0.0	0.48	0.34	0.5	4.27	2	73.3
14	0.49	0.34	0.0	0.48	0.34	0.6	4.27	2	243.3
15	0.71	0.50	0.0	0.71	0.50	0.5	6.34	3	73.4
16	0.71	0.50	0.0	0.71	0.50	0.5	5.7	3	243.3
17	0.94	0.66	0.0	0.93	0.66	0.6	8.3	3.9	73.9
18	1.02	0.72	0.0	1.01	0.71	0.6	8.78	4.1	243.3

110609

Second generator test with electromagnetic rotor

The rotor winding is made of 8 turns of 7 twisted parallel strands that are coupled in series, resulting in 56 turns, and thereby establish a conductor area on 28 mm^2 of pure copper and 21.8% fill factor. The highest excitation current, which is 10 A, gives 20 A/mm2 and more than 560 A_{turns} of magneto motive force. Remarkably a magneto motive force above 500 A_{turns} brings the rotor core into saturation.

Back EMF measurements at different excitation currents for the stator module with 15.5 turns (ST3).

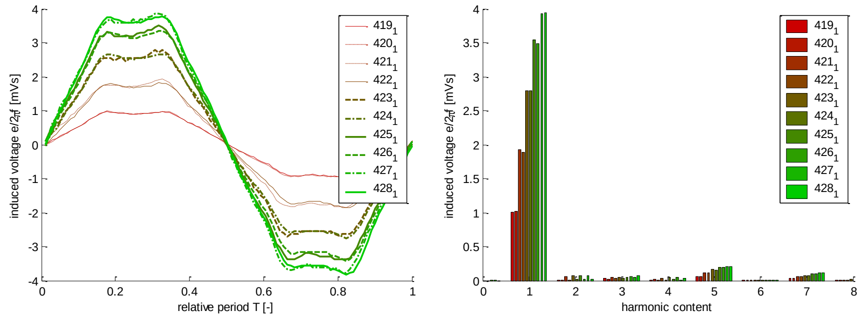

Induced voltage per excitation speed (fft, thd, rms)

Test	ψ_{m1}	ψ_{rms}	ψ_{thd}	U_{m1}	U_{rms}	U_{thd}	If	Uf	F
	mVs	mVs	%	mVs	mVs	%	A	V	Hz
19	1.01	0.71	0.0	1.01	0.71	0.6	2.11	3.8	76.2
20	1.04	0.72	0.0	1.02	0.71	0.6	2.11	3.8	245.1
21	1.94	1.36	0.0	1.92	1.35	0.6	3.97	7.3	75.3
22	1.90	1.33	0.0	1.88	1.32	0.6	3.9	7.3	244.5
23	2.82	1.98	0.0	2.79	1.96	0.5	5.84	11.3	75.3
24	2.83	1.98	0.0	2.80	1.96	0.5	5.92	11.3	244.5
25	3.58	2.51	0.0	3.54	2.49	0.5	7.54	15.6	73.6
26	3.50	2.45	0.0	3.48	2.44	0.5	7.46	15.6	244.5
27	3.97	2.78	0.0	3.92	2.75	0.4	9.97	17.5	74.3
28	3.97	2.78	0.0	3.94	2.76	0.4	10.17	17.5	245.7

110615

In a comparison of the latest results to the permanent-magnet rotor with all the magnets present, where the corresponding maximum flux linkage is 5.35 mVs, the electromagnetic rotor suffers under magnetic saturation and also shows high excitation losses (above 200W) compared to the expected output power (well below 150 W).

EMF measurements of stators with dummy windings

The target geometry of the winding is 3D-printed where the sensor coils are added. The dummy winding has two coils that are follow the profile of the coil on the innermost and outermost surface, respectively, of the winding body seen from the air-gap. The coils are placed in the middle of the corresponding surfaces as measured from the edges of the surfaces. The measurement coils each contain only a single turn. The first real winding differs from the dummy winding in that it is larger in the radial and axial direction due to the available size of the copper wire and the mounting tolerances. This leaves a slightly smaller space for the stator yoke in the mould.

The test objects are:

1. Moulded core of powder size 100-200 μm and epoxy NM FW 3070 mixed with NM 150B (ST1)

2. Moulded core of powder size 100-200 μm and epoxy Araldit LY 5052 mixed with Aradur 5052 (ST2)

3. Moulded core of “sorted and prepared” powder and epoxy Araldit LY 5052 mixed with Aradur 5052 (ST4)

4. Moulded core halves (Figure 6.4) of powder size 100-200 μm and epoxy Araldit LY 5052 mixed with Aradur 5052 (ST5)

The electrically magnetized rotor with a low field current (LC; approximately 4 A), and a high field current (HC; approximately 8 A), is driven at two different speeds: low (LS) and high (HS) speed, corresponding to 66 and 200 Hz, respectively.

High speed (HS) and low current (LC)

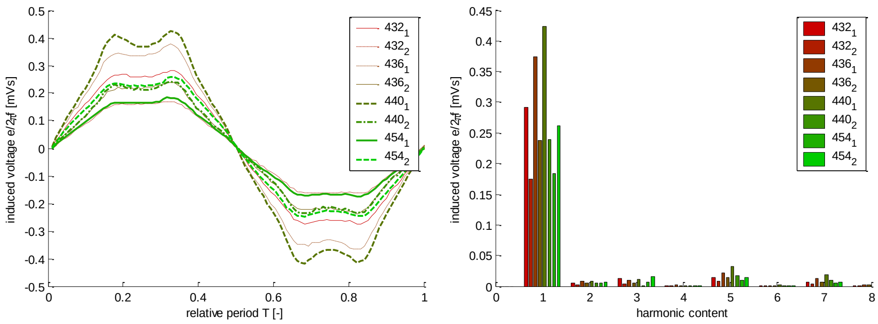

Induced voltage per excitation speed (fft, thd, rms)

Case	ψ_{m1} [mVs]	ψ_{rms} [mVs]	ψ_{TD} [%]	E_{m1}[mV]	E_{rms}, [mV]	E_{THD} [%]	Freq [Hz]	I_{field}, [A]	U_{field} [V]
ST1-LS-LC inner	0.16	0.12	0.0	0.16	0.11	0.0	67.2	4.01	7.5
ST1-LS-LC outer	0.10	0.07	0.1	0.10	0.07	0.6	67.2		
ST1-HS-LC inner	0.16	0.11	0.0	0.16	0.11	0.0	220.8	4.05	7.5
ST1-HS-LC outer	0.10	0.07	0.1	0.09	0.07	0.6	220.8		
ST1-LS-HC inner	0.30	0.21	0.0	0.28	0.21	0.0	68.8	7.96	15.0
ST1-LS-HC outer	0.18	0.13	0.0	0.17	0.12	0.4	68.8		
ST1-HS-HC inner	0.30	0.21	0.0	0.27	0.20	0.0	222.2	7.90	15.0
ST1-HS-HC outer	0.18	0.12	0.0	0.16	0.12	0.4	222.2		
ST2-LS-LC inner	0.21	0.14	0.0	0.19	0.14	0.0	68.2	4.02	7.5
ST2-LS-LC outer	0.13	0.09	0.0	0.12	0.09	0.5	68.2		
ST2-HS-LC inner	0.20	0.14	0.0	0.18	0.14	0.0	220.3	4.02	7.5
ST2-HS-LC outer	0.13	0.09	0.0	0.11	0.09	0.5	220.3		
ST2-LS-HC inner	0.39	0.27	0.0	0.33	0.27	0.0	68.1	7.93	14.9
ST2-LS-HC outer	0.24	0.17	0.0	0.21	0.17	0.6	68.1		
ST2-HS-HC inner	0.38	0.26	0.0	0.32	0.26	0.0	216.0	7.94	14.9
ST2-HS-HC outer	0.24	0.17	0.0	0.20	0.17	0.6	216.0		
ST4-LS-LC inner	0.24	0.17	0.0	0.20	0.17	0.0	67.4	4.68	7.5
ST4-LS-LC outer	0.14	0.10	0.0	0.12	0.10	0.6	67.4		
ST4-HS-LC inner	0.23	0.16	0.0	0.19	0.16	0.0	214.6	4.07	7.5
ST4-HS-LC outer	0.13	0.09	0.0	0.11	0.09	0.6	214.6		
ST4-LS-HC inner	0.42	0.30	0.0	0.33	0.29	0.0	67.1	7.85	14.9
ST4-LS-HC outer	0.24	0.17	0.0	0.19	0.17	0.6	67.1		
ST4-HS-HC inner	0.43	0.30	0.0	0.33	0.30	0.0	209.6	7.90	14.9
ST4-HS-HC outer	0.24	0.17	0.0	0.18	0.17	0.7	209.6		
ST5-LS-LC inner	0.15	0.10	0.1	0.14	0.10	0.8	67.1	4.05	7.5
ST5-LS-LC outer	0.10	0.07	0.0	0.10	0.07	0.0	67.1		
ST5-HS-LC inner	0.14	0.10	0.1	0.14	0.10	0.8	213.2	4.12	7.5
ST5-HS-LC outer	0.10	0.07	0.0	0.10	0.07	0.0	213.2		
ST5-LS-HC inner	0.27	0.19	0.0	0.26	0.19	0.6	68.6	8.00	15.0
ST5-LS-HC outer	0.19	0.13	0.0	0.19	0.13	0.0	68.6		
ST5-HS-HC inner	0.26	0.18	0.1	0.26	0.18	0.7	213.7	7.96	15.0
ST5-HS-HC outer	0.19	0.13	0.0	0.18	0.13	0.0	213.7		

110628 and 110630

The measurement results are comparable to the real winding when considering 15.5 winding turns instead of one. The values for the real winding usually lie between those for the inner and the outer test coils. The following observations can be made:

1. The moulding process and the quality of the binder have a remarkable influence on the magnetic characteristics of the core.

2. The difference between the 100-200 μm powder and the “sorted and prepared” powder is relatively small, and is more noticeable in the inner (“near”) test coil than in the outer (“far”) test coil. This may rather be to do with the unpredictability of the magnetic properties of the moulded core.

3. The stator made of two halves shows a smaller difference between the near and far sensor coils and also considerably lower values in the near coil. This could be due to the moulding and the additional small air gaps.

Stator made of compact coils and core halves

A new compact coil is created with 12 turns. The coil is mounted between two identical core halves that might have an additional small air gap in the axial direction. As the first experimental core halves are produced from separate parts — the main core with teeth and yoke integrated, along with a number of tooth-tips — the speculative question of the real magnetic permeability in different parts cannot be answered. Furthermore there is an additional small air gap between the main core and the tooth-tips.

Back EMF measurements at different excitation currents for the stator module with 12 turns (ST5) are recalculated to 15.5 turns in order to make the measurements easily comparable to previous results (ST3).

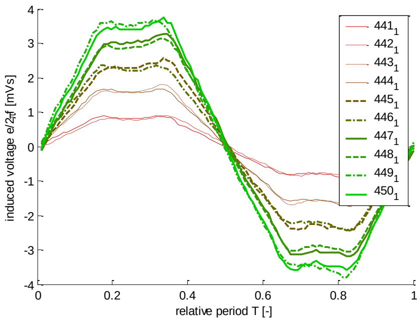

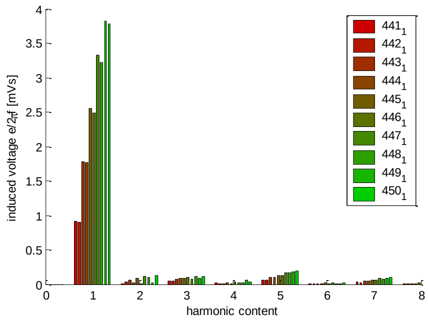

Induced voltage per excitation speed (fft, thd, rms)

Test	ψ_{m1}	ψ_{rms}	ψ_{thd}	U_{m1}	U_{rms}	U_{thd}	If	Uf	F
	mVs	mVs	%	mVs	mVs	%	A	V	Hz
41	0.92	0.65	0.1	0.91	0.64	0.8	2.0	3.6	64.9
42	0.90	0.63	0.1	0.90	0.64	0.8	1.96	3.6	165.6
43	1.80	1.26	0.1	1.78	1.25	0.7	4.02	7.4	66.2
44	1.79	1.25	0.1	1.77	1.24	0.7	4.05	7.5	166.7
45	2.59	1.81	0.1	2.55	1.79	0.6	6.06	11.0	65.3
6	2.50	1.75	0.1	2.48	1.74	0.6	6.03	11.0	164.7
47	3.36	2.35	0.1	3.33	2.34	0.5	8.21	15.1	65.4
48	3.25	2.28	0.1	3.22	2.26	0.5	8.01	15.0	169.8
49	3.86	2.70	0.0	3.82	2.68	0.5	9.85	18.5	63.9
50	3.83	2.68	0.0	3.78	2.65	0.5	9.83	18.5	188.3

110629

The difference between the actual moulded winding segments is relatively small compared to moulded dummy windings. When considering the single-piece moulded core and the stator made of two core halves, the results are similar. The explanation could be that the newest compacted winding is near to the desired winding geometry that leaves more space for the stator yoke, compared to the first winding that is moulded into the core.

Remarks on further development

A number of aspects can be discussed concerning further development.

1. Stator core: The magnetic permeability of the core or core parts must be increased in order to improve the performance of the machine. As the implementation of the core halves gives results comparable to the complete one-step moulded core, which is so far to do with the more ideal winding shape as it gives a smaller mounting tolerance. It is worth considering adding magnetic high-permeability inserts to improve the magnetic coupling. It is also expected that the high-permeability core parts with well-defined magnetic properties will reduce the sensitivity of the material properties related to the moulding process or even the material inputs to the process.

2. Rotor core: It is wise to investigate the geometry and material properties in order to reduce the magnetic overloading that brings the core to saturation. Currently, the low compacted winding brings the core to saturation, and it would be worth considering reducing the winding slot area by increasing the core rather than by improving the compaction of the rotor winding. Another suggestion would be to investigate the rotor core by using magnetic bandage and field sensor alone, in order to focus on the magnetic characteristics of electrically magnetized rotor only when evaluating the relation between the magnetic flux and the excitation current.

3. Stator and rotor windings: It is worth increasing the conductor fill factor to make the copper/conductor losses smaller; as the copper volume grows the DC losses becomes lower, as the resistive losses are the resistance multiplied by the square of the current density. The risk of high fill factor is that the mounting tolerances will grow faster and the size of the winding will become considerably larger, having an impact on the final size of the magnetic core.

Symbol list

Ac1	Material in the stator core.
Acu	Stator winding cross section area.
Ai1	Insulation area stator slot.
Aw1	The stator winding cross section area.
Bc1	Material in the rotor core.
Bi1	Insulation area rotor slot.
Bw1	The rotor winding cross section area.
C	Capacitance.
CuRW	Rotor winding width.
CuSW	Stator winding width.
Em1	EMF fundamental peak value
EMF	Electromagnetic force.
EMSM	Electric magnetized synchronous machine.
E_{rms}	Electromagnetic force root mean square.
E_{THD}	Total harmonic distortion.
f	frequency.
FEMM	Finite element method magnetics.
Iscc	Current in stator closed circuit.
$\hat{\imath}_w$	Maximum peek current in a phase.
$\hat{\jmath}_{cd}$	Current density in stator winding.
Ks	Relative stator/rotor slot width defined as slot width divided by slot pitch.
Ky	Relative stator/rotor radial slot length.
L	Inductance.
M235-35A	Laminated sheets from Surahammar Bruks AB
N	Number of stator winding turns.
n	Efficiency.
N-slots	Number of slots.
N-turns	number of winding turns.
Np	Number of poles.
Ns	Number of slots.
Pcu	current losses in stator/rotor winding.
P_f stator	Losses in the stator winding.

Pin	Power in to the machine.
Put	Output power on the axes.
POM-C	A thermo plastic polymer.
R	Resistance.
Rpm	Revolutions per minute.
SMC	Soft magnetic composite.
SM^2C	Soft magnetic mouldable composite.
SM^2C-G	Soft magnetic mouldable composite gravitational moulding.
SM^2C-I	Soft magnetic mouldable composite initial material properties.
SM2C-R	Rotocasted soft magnetic mouldable composite.
Som-3P	Somaloy from Höganäs AB.
Som-5P	Somaloy from Höganäs AB.
St'nr'	Stator winding configuration test.
Tmax	Maximum torque in a simulation.
TFM	Transversal flux machine (claw pole machine).
Uoc	Voltage open circuit.
μr	Relative permeability.
W-type	Winding type.
π	Pi.
Ψ_{m1}	Flux linkage fundamental peak value
Ψ_{rms}	Linked flux root mean square.
Ψ_{thd}	Flux linkage total harmonic distortion